Gastroenterology 2020;■:1–17

ABL1, Overexpressed in Hepatocellular Carcinomas, Regulates Expression of NOTCH1 and Promotes Development of Liver Tumors in Mice

Fang Wang,[1,2,*] **Wei Hou**,[1,2,*] Lennox Chitsike,[1,2] Yingchen Xu,[3] Carlee Bettler,[1,2] Aldeb Perera,[1,2] Thomas Bank,[1,2] Scott J. Cotler,[4] Asha Dhanarajan,[5] Mitchell F. Denning,[5] Xianzhong Ding,[5] Peter Breslin,[6,7,8] Wenan Qiang,[9] Jun Li,[10] Anthony J. Koleske,[11] and Wei Qiu[1,2]

[1]Department of Surgery, Loyola University Chicago Stritch School of Medicine, Chicago, Illinois; [2]Department of Cancer Biology, Loyola University Chicago Stritch School of Medicine, Chicago, Illinois; [3]Department of General Surgery, Beijing Tongren Hospital, Capital Medical University, Beijing, China; [4]Department of Medicine, Loyola University Chicago Stritch School of Medicine, Chicago, Illinois; [5]Department of Pathology, Loyola University Chicago Stritch School of Medicine, Chicago, Illinois; [6]Department of Molecular/Cellular Physiology, Loyola University Chicago Stritch School of Medicine, Chicago, Illinois; [7]Oncology Institute, Loyola University Chicago Stritch School of Medicine, Chicago, Illinois; [8]Department of Biology, Loyola University Chicago Stritch School of Medicine, [9]Department of Obstetrics and Gynecology and Pathology, Northwestern University, Chicago, Illinois; [10]Department of Applied and Computational Mathematics and Statistics, University of Notre Dame, Notre Dame, Indiana; and [11]Department of Molecular Biophysics and Biochemistry, Yale University, New Haven, Connecticut

BACKGROUND & AIMS: We investigated whether ABL proto-oncogene 1, non-receptor tyrosine kinase (ABL1) is involved in development of hepatocellular carcinoma (HCC). **METHODS:** We analyzed clinical and gene expression data from The Cancer Genome Atlas. *Albumin*-Cre (Hep^{WT}) mice and mice with hepatocyte-specific disruption of *Abl1* ($Hep^{Abl-/-}$ mice) were given hydrodynamic injections of plasmids encoding the Sleeping Beauty transposase and transposons with the MET gene and a catenin β1 gene with an N-terminal truncation, which induces development of liver tumors. Some mice were then gavaged with the ABL1 inhibitor nilotinib or vehicle (control) daily for 4 weeks. We knocked down *ABL1* with short hairpin RNAs in Hep3B and Huh7 HCC cells and analyzed their proliferation and growth as xenograft tumors in mice. We performed RNA sequencing and gene set enrichment analysis of tumors. We knocked down or overexpressed NOTCH1 and MYC in HCC cells and analyzed proliferation. We measured levels of phosphorylated ABL1, MYC, and NOTCH1 by immunohistochemical analysis of an HCC tissue microarray. **RESULTS:** HCC tissues had higher levels of ABL1 than non-tumor liver tissues, which correlated with shorter survival times of patients. Hep^{WT} mice with the MET and catenin β1 transposons developed liver tumors and survived a median 64 days; $Hep^{Abl-/-}$ mice with these transposons developed tumors that were 50% smaller and survived a median 81 days. Knockdown of ABL1 in human HCC cells reduced proliferation, growth as xenograft tumors in mice, and expression of MYC, which reduced expression of NOTCH1. Knockdown of NOTCH1 or MYC in HCC cells significantly reduced cell growth. NOTCH1 or MYC overexpression in human HCC cells promoted proliferation and rescued the phenotype caused by ABL1 knockdown. The level of phosphorylated (activated) ABL1 correlated with levels of MYC and NOTCH1 in human HCC specimens. Nilotinib decreased expression of MYC and NOTCH1 in HCC cell lines, reduced the growth of xenograft tumors in mice, and slowed growth of liver tumors in mice with MET and catenin β1 transposons, reducing tumor levels of MYC and NOTCH1. **CONCLUSIONS:** HCC samples have increased levels of ABL1 compared with nontumor liver tissues, and increased levels of ABL1 correlate with shorter survival times of patients. Loss or inhibition of ABL1 reduces proliferation of HCC cells and slows growth of liver tumors in mice. Inhibitors of ABL1 might be used for treatment of HCC.

Keywords: Hepatocarcinogenesis; Mouse Model; Signal Transduction; Oncogene.

Hepatocellular carcinoma (HCC) is the major form of liver cancer. It is the sixth most common malignancy globally and ranks fourth in total cancer-related deaths annually.[1] The 5-year overall survival of patients with a new diagnosis of HCC is <18%, and a majority of HCC patients present with advanced disease, so treatment options are limited.[2] Currently, first-line therapeutic agents for advanced HCC, either sorafenib or lenvatinib, increase survival by only approximately 3 months.[3] Recently a number of drugs, including regorafenib, cabozantinib, and nivolumab, have been approved by the US Food and Drug Administration for second-line treatment of HCC.[3] However, these drugs only offer a further increase in overall survival of 3–5 months. Therefore, it is imperative to develop new and more effective therapeutic strategies and agents to treat

*Authors share co-first authorship.

Abbreviations used in this paper: **ABL1, Abelson tyrosine-protein kinase 1; CAT, constitutively active β-catenin; GSEA, gene set enrichment analysis; HCC, hepatocellular carcinoma; IHC, immunohistochemical; KD, knockdown; miR, microRNA; mRNA, messenger RNA; shRNA, short hairpin RNA; TCGA, The Cancer Genome Atlas; TUNEL, terminal deoxynucleotidyl transferase–mediated deoxyuridine triphosphate nick-end labeling.**

0016-5085/$36.00
https://doi.org/10.1053/j.gastro.2020.03.013

WHAT YOU NEED TO KNOW

BACKGROUND AND CONTEXT

The oncogene ABL1 might be involved in the pathogenesis of hepatocellular carcinoma (HCC).

NEW FINDINGS

HCC samples have increased levels of ABL1 compared with non-tumor liver tissues, and loss or inhibition of ABL1 reduces proliferation of HCC cells and slows growth of tumors in mice.

LIMITATIONS

This study was performed using human tissue samples, cell lines, and mice. Further studies in humans are needed.

IMPACT

Inhibitors of ABL1 might be developed for treatment of HCC

HCC, but achieving this goal requires a better understanding of the molecular signaling pathways that drive or mediate the development of the disease.

Abelson tyrosine-protein kinase 1 (ABL1) is a non-receptor tyrosine kinase of the Abelson-like family. It is mostly known for its involvement in leukemias harboring the Philadelphia chromosome, which results from the translocation of the short arms of chromosomes 9 and 22, creating a fusion of the *BCR* gene to the second exon of the *ABL1* gene, resulting in the production of the BCR-ABL fusion protein.[4] Recent evidence has shown that ABL1 also plays an important role in the development of solid tumors, such as melanoma, breast cancer, ovarian cancer, and lung cancer, by an independent mechanism not involving any fusion oncoproteins.[4] We previously reported that ABL1 is overexpressed and activated in human HCC specimens.[5] However, the role of ABL1 in hepatocarcinogenesis must be understood because it is critical for determining whether ABL1 is a suitable candidate target in the treatment of HCC.

We report that overexpression of ABL1 correlates with poor prognosis in HCC. We investigated the role of ABL1 in HCC growth using in vitro and mouse models. We found that *ABL1* inhibition impaired HCC growth and extended overall survival of mice with HCC. Mechanistically, we found that inhibition of ABL1 suppresses HCC cell growth by decreasing *NOTCH1* expression through the regulation of c-MYC. Collectively, our data strongly suggest that ABL1 is involved in the pathogenesis of HCC and that its inhibition could be a promising novel strategy to treat this disease.

Methods

Cells and Treatments

Huh7 cells were purchased from JCRB Cell Bank (Osaka, Japan). Hep3B, Skep1, SNU423, SNU449, SNU475, PLC/PRF, SNU387, and 293T cells were purchased from ATCC (Manassas, VA). All cells were cultured as described previously.[6]

For knockdown experiments, Huh7 and Hep3B cells were infected with lentiviral pLKO.1 particles, which contain *ABL1*, *NOTCH1*, *c-MYC*, or scrambled short hairpin RNA (shRNA) and selected with 2 μg/mL puromycin for 5 days. Lentiviral pLKO.1 plasmids for sh*ABL1* (Supplementary Table 1), sh*NOTCH1* (Supplementary Table 1), sh*c-MYC*,[7] or scrambled shRNA (SHC002; Sigma-Aldrich, St Louis, MO) were packaged with pCMV-dr8.2 (Addgene, Watertown, MA) and pCMV-VSVG (Addgene) in 293T cells to produce lentiviral particles, as described previously.[7]

For NOTCH1 overexpression experiments, the NOTCH1 (NOTCH intercellular domain) expression plasmid (EF.hICN1.CMV.GFP), purchased from Addgene (#17623), was packaged with CMV-dr8.2 and pCMV-VSVG in 293T cells to produce lentiviral particles. Six days after infection with the lentiviral particles, GFP-positive scrambled and *ABL1* knockdown (KD) Huh7 cells expressing NOTCH1 were sorted by flow cytometry (FACSAria Cell Sorter; BD Biosciences, San Jose, CA). The proliferation of these cells was then analyzed using alamarBlue assay, as described previously.[6]

For experiments involving the overexpression of c-MYC, the pBpuro c-MycER retroviral plasmid (gifted from Dr Gerard Evan)[8] and control pBpuro retroviral plasmids (Addgene, #1764) were packaged with pMD.MLV and pMD.G/pVSV.G in 293T cells to produce retroviral particles. Six days after infection with the retroviral particles, scrambled and *ABL1*-KD Huh7 cells were treated with 100 nM 4-hydroxytamoxifen. The proliferation of these cells was then analyzed using alamarBlue assay.

For ABL inhibitor experiments, HCC cells were seeded into 96-well plates. After 24 hours in culture, the cells were treated with nilotinib (LC Laboratories, Woburn, MA; cat #N-8207) (1–20 μM) or GNF-5 (Selleckchem, Houston, TX; cat #S7526) (1–20 μM); cell proliferation was then analyzed using either SRB[9] or alamarBlue assay after 48 or 72 hours.

Mice and Treatments

All animals received humane care according to the Guide for the Care and Use of Laboratory Animals. The procedures for all animal experiments detailed were approved by the Institutional Animal Care and Use Committee of Loyola University Chicago. All mice were housed in micro-isolator cages in a room illuminated from 7:00 AM to 7:00 PM (12:12-hour light–dark cycle) and were given access to water and chow ad libitum.

To generate mice with hepatocyte-specific *Abl1*-deficiency, *Abl1*$^{flox/flox}$ mice (Jackson Laboratory, Bar Harbor, ME; cat #013224) were backcrossed to C57BL/6J mice for 5 generations and then were mated with *Albumin*-Cre mice (Jackson Laboratory; cat #003574). The resulting offspring *Alb*-Cre; *Abl1*$^{flox/+}$ mice were then mated to generate the *Albumin*-Cre and Alb-Cre; *Abl1*$^{flox/flox}$ littermates. The age- (6–8 weeks old) and sex-matched *Albumin*-Cre and Alb-Cre; *Abl1*$^{flox/flox}$ mice were injected with plasmids, encoding the Sleeping Beauty transposase (HSB2) and transposons with GFP (pT3-GFP) or MET gene and catenin β1 gene with the N-terminal truncation (referred to here as MET/CAT), as described previously.[10]

Four weeks after MET/CAT injection, C57BL/6J wild-type mice were given with vehicle (30% captisol), nilotinib (20 mg/kg) or sorafenib (25 mg/kg) by oral gavage daily for 4 weeks or before being sacrificed (some mice treated with vehicle had to be euthanized earlier due to tumor burdens). Age- and sex-matched mice were allocated to different

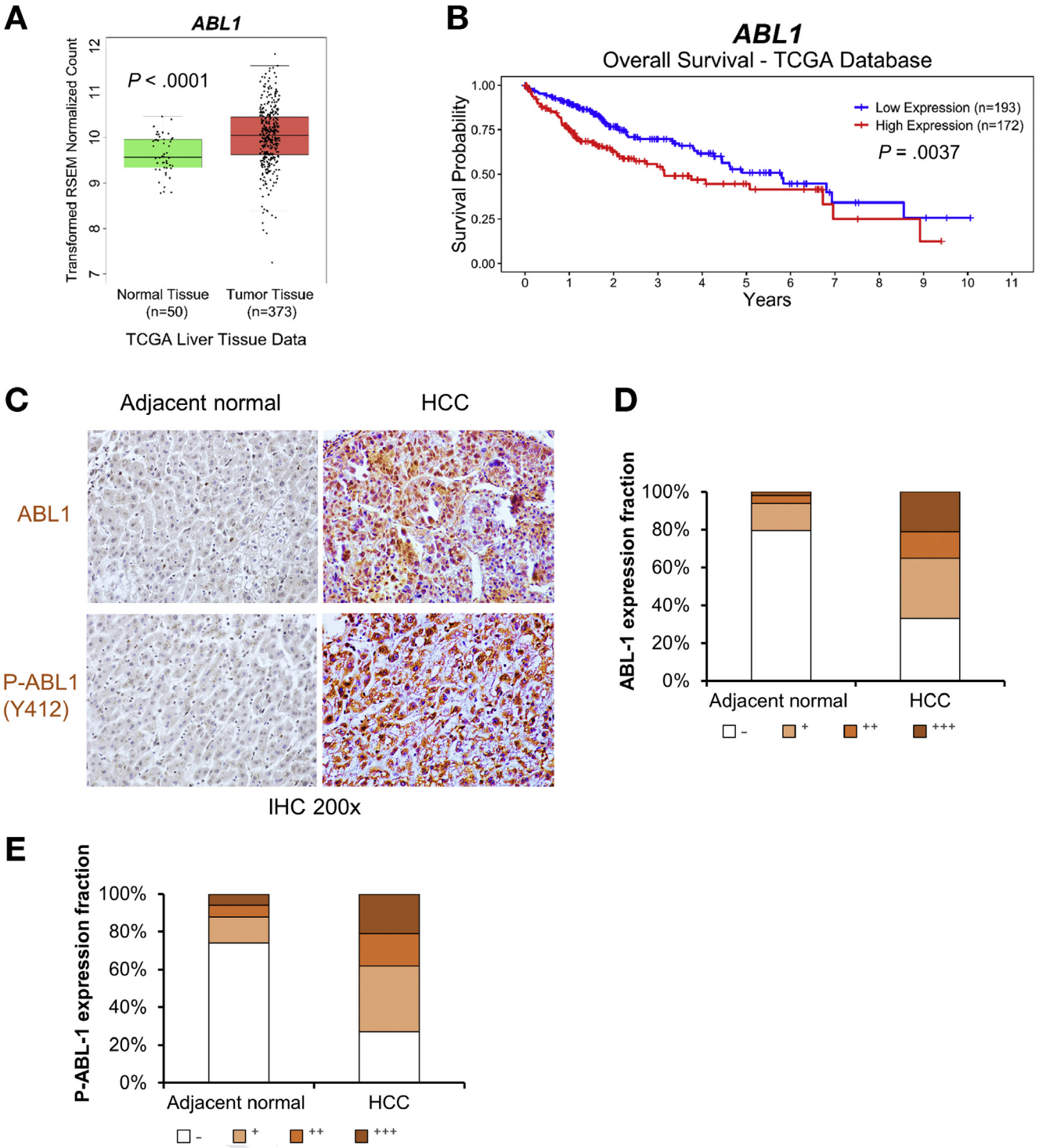

Figure 1. High expression of *ABL1* in human HCCs is positively correlated with shorter patient survival times. (*A*) Relative expression of *ABL1* mRNA in normal liver and HCC specimens from TCGA database. (*B*) *ABL1* mRNA expression is correlated with shorter survival times in HCC patients. (*C*) Representative photos of ABL1 and p-ABL1 IHC staining in adjacent normal liver and HCC specimens from tissue microarrays. (*D, E*) Quantification of ABL1 and p-ABL1 IHC staining from tissue microarrays (66 cases of HCC and 50 normal tissue specimens).

treatment groups. Both male and female mice were used in the experiments. Six- to-eight-week-old mice were used for hydrodynamic injections.

Xenograft model. Huh7 cells (5×10^6 in 100 μL serum-free medium) were injected into the left or right flanks of the 8- to 12-week-old SCID-bg mice. Three weeks post-injection, some mice were given with vehicle (30% captisol) or nilotinib (20 mg/kg) by oral gavage daily for 10 days. Tumor volumes were measured daily using a caliper until the day of sacrifice.

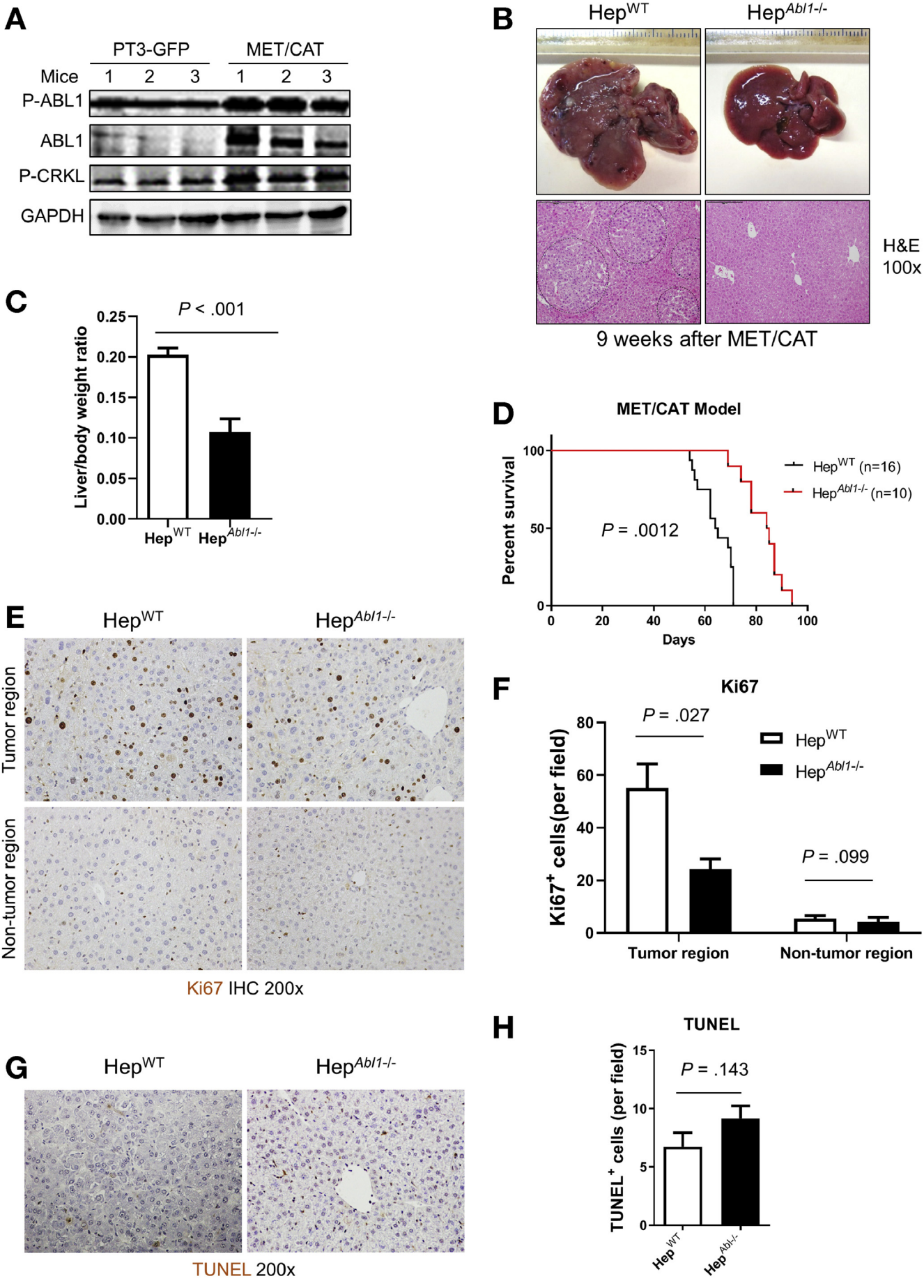

Western Blotting

Western blotting was performed as described previously.[6] Information on primary antibodies is provided in Supplementary Table 2.

Quantitative Real-Time Polymerase Chain Reaction

Cellular or tissue messenger RNA (mRNA) was extracted using Zymo mini-columns and quantitative real-time polymerase chain reactions were performed as described previously.[6] Primers used for real-time polymerase chain reaction are listed in Supplementary Table 3.

Immunohistochemical Staining

IHC was performed as described previously.[10] Human tissue microarrays LV801, LV807, and LV8012 were purchased from US Biomax (Rockville, MD). LV801 and LV807 contain a total of 66 cases of HCC and 50 cases of HCC adjacent normal or normal liver tissues. LV8012 contains 80 cases of HCC (TNM stage II–IV). The IHC signals were quantified visually. The staining was scored as − (0, negative), + (1, weak signal), + + (2, moderate signal), and + + + (3, strong signal) by 2 independent observers, including a pathologist from Loyola University Chicago; a sample was rated as positive if it showed at least 1% of cells with a staining score ≥1+. For IHC on mouse samples, cells with positive staining were scored in at least 5 fields at 400× or 200× magnification and reported as mean ± SD. Information on primary antibodies for IHC is provided in Supplementary Table 2.

Terminal Deoxynucleotidyl Transferase–Mediated Deoxyuridine Triphosphate Nick-End Labeling Staining

Terminal deoxynucleotidyl transferase–mediated deoxyuridine triphosphate nick-end labeling (TUNEL) staining was performed as described previously.[6] The TUNEL-positive cell number was scored in at least 5 fields at 400× magnification/mouse and reported as mean ± SD. Three or more mice were used in each group.

RNA Sequencing and Analysis

RNA from scrambled control and *ABL1*-KD Huh7 cells was extracted using RNeasy Plus Micro Kit (Qiagen, Germantown, MD). RNA sequencing was performed by Novogene Corporation (Hong Kong). Gene set enrichment analysis (GSEA) was performed using the 3.0 GSEA software. The RNA sequencing data were deposited into the National Center for Biotechnology Information's Gene Expression Omnibus database (GEO GSE133294. https://www.ncbi.nlm.nih.gov/geo/query/acc.cgi?acc=GSE133294).

Chromatin Immunoprecipitation Assay

Huh7 cell were cultured as described above and chromatin immunoprecipitation assays were performed as described previously[11] using a c-MYC antibody (#5605; Cell Signaling, Danvers, MA). The primers used are listed in Supplementary Table 3.

Proximity Ligation Assay

Proximity ligation assay was performed using the Duolink In Situ Red Starter Kit Mouse/Rabbit (MilliporeSigma, Burlington, MA) according to the manufacturer's instructions. Details are provided in the Supplementary Material.

Human Sample Analysis

Alterations of *ABL1*, *NOTCH1*, and *c-MYC* mRNA were analyzed from publicly available data from The Cancer Genome Atlas (TCGA).[12] Analysis of gene expression, Kaplan-Meier survival analyses, and correlations were performed using R, version 3.6.0, Python, version 3.0, and GraphPad Prism, version 8.0 (GraphPad, San Diego, CA) software. Details are provided in the Supplementary Material.

Statistical Analysis

Statistical analyses were performed using GraphPad Prism software, version 8.0. Variation is indicated using standard error presented as mean ± SD. Statistical significance was calculated using the 2-tailed Student *t* test, except for the experiments involving repeated measures, which were analyzed using 2-way analysis of variance. $P < .05$ was considered significant. Means ± SDs are shown in the Figures where applicable.

Results

High Expression of ABL1 in Human Hepatocellular Carcinomas Is Positively Correlated With Shorter Survival Times of Patients

We previously reported that ABL1 is overexpressed in human HCC specimens with a small sample size.[5] To confirm the results with a larger sample size, we analyzed the TCGA database and confirmed that *ABL1* was expressed at higher levels in HCCs compared to normal liver tissues (Figure 1*A*). In addition, we found that higher *ABL1* expression is positively correlated with poorer prognosis in human HCC patients from the TCGA database (Figure 1*B*

Figure 2. Deletion of *Abl1* suppresses tumor development and prolongs survival in the MET/CAT-induced HCC mouse model. (*A*) Levels of p-ABL1 (p-Y412), ABL1, p-CRKL and GAPDH proteins in the livers of Hep^{WT} mice 9 weeks after hydrodynamic injection of MET/CAT or pT3-GFP. (*B*) Photographs and H&E staining of livers of Hep^{WT} and $Hep^{Abl1-/-}$ mice 9 weeks after injection of MET/CAT. (*C*) Liver body/weight ratios were analyzed in the mice from (*B*) (n = 6). (*D*) Survival curves of Hep^{WT} and $Hep^{Abl1-/-}$ mice after injection of MET/CAT. (*E*) Hepatocyte proliferation of Hep^{WT} and $Hep^{Abl1-/-}$ mice 9 weeks after injection of MET/CAT was examined by immunohistochemistry for Ki67. (*F*) Quantification of Ki67 staining for (*E*) (n = 4). (*G*) Apoptosis in the livers of Hep^{WT} and $Hep^{Abl1-/-}$ mice 9 weeks after injection of MET/CAT was examined by TUNEL staining. (*H*) Quantification of TUNEL staining for (*G*) (n = 4).

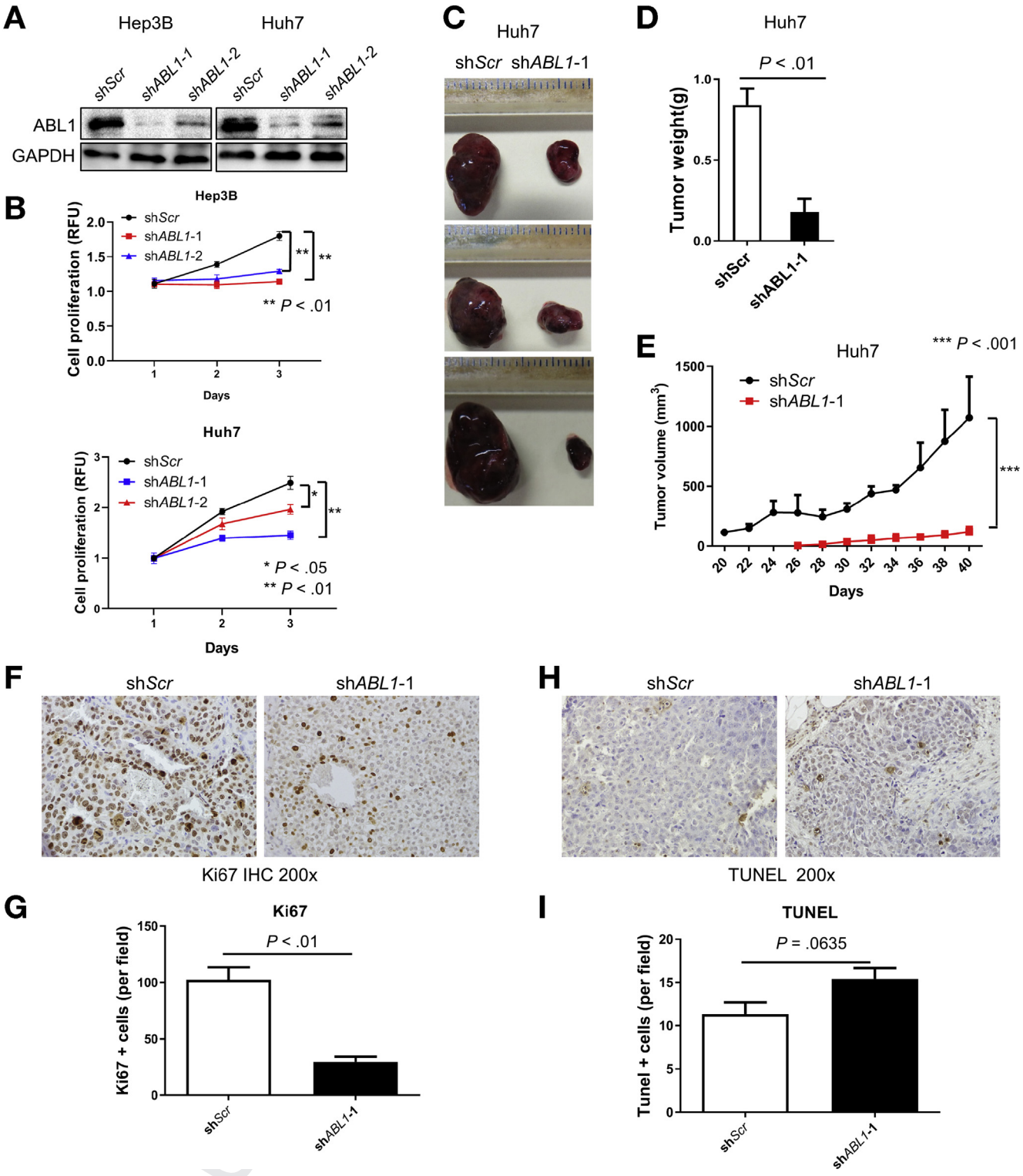

Figure 3. ABL1 knockdown reduces human HCC cell proliferation and suppresses tumor growth. (*A*) ABL1 and GAPDH protein expression in scrambled-RNA and ABL1-KD Hep3B and Huh7 cells was determined by Western blotting. (*B*) Quantification of cell proliferation from scrambled-RNA and ABL1-KD Hep3B and Huh7 cells at different time points after seeding. (*C*) SCID-bg mice were injected on their flanks with scrambled-RNA (*left*) and ABL1-KD Huh7 cells (*right*); after 40 days, *gross images* of tumors are shown. (*D*) Tumor weight from scrambled-RNA and ABL1-KD Huh7 cell-injected mice (n = 5). (*E*) Tumor volumes from scrambled-RNA and ABL1-KD Huh7 cell-injected mice (n = 5/group). (*F*) Ki67 staining of the tumors was examined by IHC. (*G*) Quantification of Ki67 staining. (*H*) Apoptosis of the tumors was examined by TUNEL staining. (*I*) Quantification of TUNEL staining.

and Supplementary Figure 1), which suggests that it could be a good prognostic factor. We also performed 2 additional HCC tissue microarrays, which contain 66 cases of HCC and 50 cases of HCC adjacent normal or normal liver tissues. Consistent with previous results,[5] we found that ABL1 protein levels were significantly higher in tumors compared to normal liver tissues (Figure 1*C* and *D*). Kinase activity is critical for the functions of ABL1.[13] Phosphorylation of Tyr412, which is located in the kinase activation loop of ABL1, is required for its kinase activity.[14,15] We found that the level of p-ABL1 (p-Tyr412) is largely absent in normal liver tissues, but is abundant in HCC specimens (Figure 1*C* and *E*). It is notable that 86% of HCC specimens with high p-ABL1 (p-Tyr412) staining also express high levels of ABL1 (Figure 1*D* and *E*). In general, these data indicate that ABL1 is overexpressed and activated in human HCCs, and that these factors correlate with shorter survival times of patients.

Deletion of Abl1 *in Hepatocytes Does Not Affect Morphology, Histology, Proliferation, or Apoptosis in Mouse Livers*

To investigate the role of ABL1 in liver tumorigenesis, we generated mice with hepatocyte-specific deletion of *Abl1* (*Albumin*-Cre; $Abl1^{flox/flox}$). *Albumin*-Cre; $Abl1^{flox/flox}$ mice (referred to here as $Hep^{Abl1-/-}$) express Cre recombinase from the albumin promoter, which is specifically expressed in hepatocytes. $Hep^{Abl1-/-}$ mice are viable, fertile, and visually indistinguishable from wild-type (*Albumin*-Cre, referred to here as Hep^{WT}) mice, suggesting that *Abl1* is not required for normal liver development. We confirmed that Cre recombinase expression in hepatocytes removes the *Abl1* allele between 2 loxP sites (Supplementary Figure 2*A*) and showed that ABL1 expression was decreased in both whole liver tissue and hepatocytes (Supplementary Figure 2*B*). There was no significant difference in morphology or histology of livers between Hep^{WT} and $Hep^{Abl1-/-}$ mice (Supplementary Figure 2*C* and *D*). Furthermore, *Abl1* deficiency did not affect cell proliferation or apoptosis in mouse livers (Supplementary Figure 2*E*–*H*). These results suggest that deletion of *Abl1* in hepatocytes does not affect mouse liver homeostasis.

Deficiency of Abl1 *in Hepatocytes Suppresses MET/CAT-Induced Hepatocellular Carcinoma Development*

MET can bind directly to ABL1 and activate it in mouse mammary tumors and breast cancer cells.[16] To determine the role of ABL1 in HCC development, we used the MET (MET)/β-catenin (CAT)-driven HCC model, which is useful for studying the functions of genes in hepatocarcinogenesis because of its clinical relevance and efficiency of HCC induction.[10,17] We found that levels of phosphorylation of both ABL1 on Tyr412 and CRKL, a direct target of ABL kinases[18] commonly used to assess ABL kinase activity, was increased in MET/CAT-induced liver tumors, suggesting that ABL1 is activated in MET/CAT-induced HCC (Figure 2*A*). Expression of ABL1 was also increased in MET/CAT-induced liver tumors (Figure 2*A*). In contrast, expression or phosphorylation of ABL1 was not altered in the diethylnitrosamine-induced HCC model (Supplementary Figure 3). These observations suggest that the MET/CAT model is suitable for studying the role of ABL1 in hepatocarcinogenesis. We hydrodynamically injected age- and sex-matched Hep^{WT} and $Hep^{Abl1-/-}$ mice with plasmids encoding the Sleeping Beauty transposase (HSB2) and transposons with the *MET/CAT* oncogenes. Comparable transfection efficiency was observed in wild-type and *Abl1* KO mouse livers (Supplementary Figure 4). Intriguingly, we found that the overall tumor load and tumor sizes in $Hep^{Abl1-/-}$ mice was decreased significantly compared to Hep^{WT} mice (Figure 2*B*). The relative liver weight, including tumor vs body weight, in $Hep^{Abl1-/-}$ mice was decreased by 50% compared to Hep^{WT} mice (Figure 2*C*). Importantly, the Hep^{WT} mice with a liver tumor burden died at the age of 55–70 days (median survival 64 days) compared to a median survival of 81 days in $Hep^{Abl1-/-}$ mice (Figure 2*D*). These data indicate that *Abl1* deficiency in hepatocytes suppresses MET/CAT-induced HCC growth and prolongs survival of mice with HCC.

ABL1 regulates cell survival and proliferation.[4] Suppression of HCC development by the deletion of *Abl1* could be due to increased apoptosis or decreased proliferation of tumor cells. We first analyzed proliferation in the MET/CAT-injected livers from Hep^{WT} and $Hep^{Abl1-/-}$ mice by Ki67 staining. The number of Ki67-positive cells was significantly decreased in tumors but not in tumor-free areas in *Abl1*-deficient livers compared to wild-type livers (Figure 2*E* and *F*). We did not find significant differences in apoptosis in livers of Hep^{WT} mice compared to those of $Hep^{Abl1-/-}$ mice (Figure 2*G* and *H*). These results demonstrate that *Abl1* deficiency in hepatocytes decreases tumor cell proliferation but not cell survival in MET/CAT-induced HCC.

Knockdown of ABL1 *Reduces Human Hepatocellular Carcinoma Cell Proliferation and Suppresses Tumor Growth*

We further investigated the role of ABL1 in human HCC. To achieve this goal, we used shRNA to knock down ABL1 expression in 2 HCC cell lines that show high levels of *ABL1* mRNA, Hep3B, and Huh7 (Supplementary Figure 5). Western blotting showed that ABL1 was successfully knocked down by 2 shRNAs in both cell lines (Figure 3*A*). Importantly, knockdown of ABL1 significantly reduced cell growth in both Hep3B and Huh7 cells (Figure 3*B*). Consistently, ABL1 knockdown decreased growth as xenograft tumors in mice (Figure 3*C*–*E*). Tumors grown from ABL1-KD cells also displayed less cell proliferation compared to those grown from scrambled-RNA control cells (Figure 3*F* and *G*). However, there was no significant difference in apoptosis in tumors from the 2 groups (Figure 3*H* and *I*). Collectively, these results indicate that knockdown of ABL1 reduces human HCC cell proliferation and suppresses tumor growth.

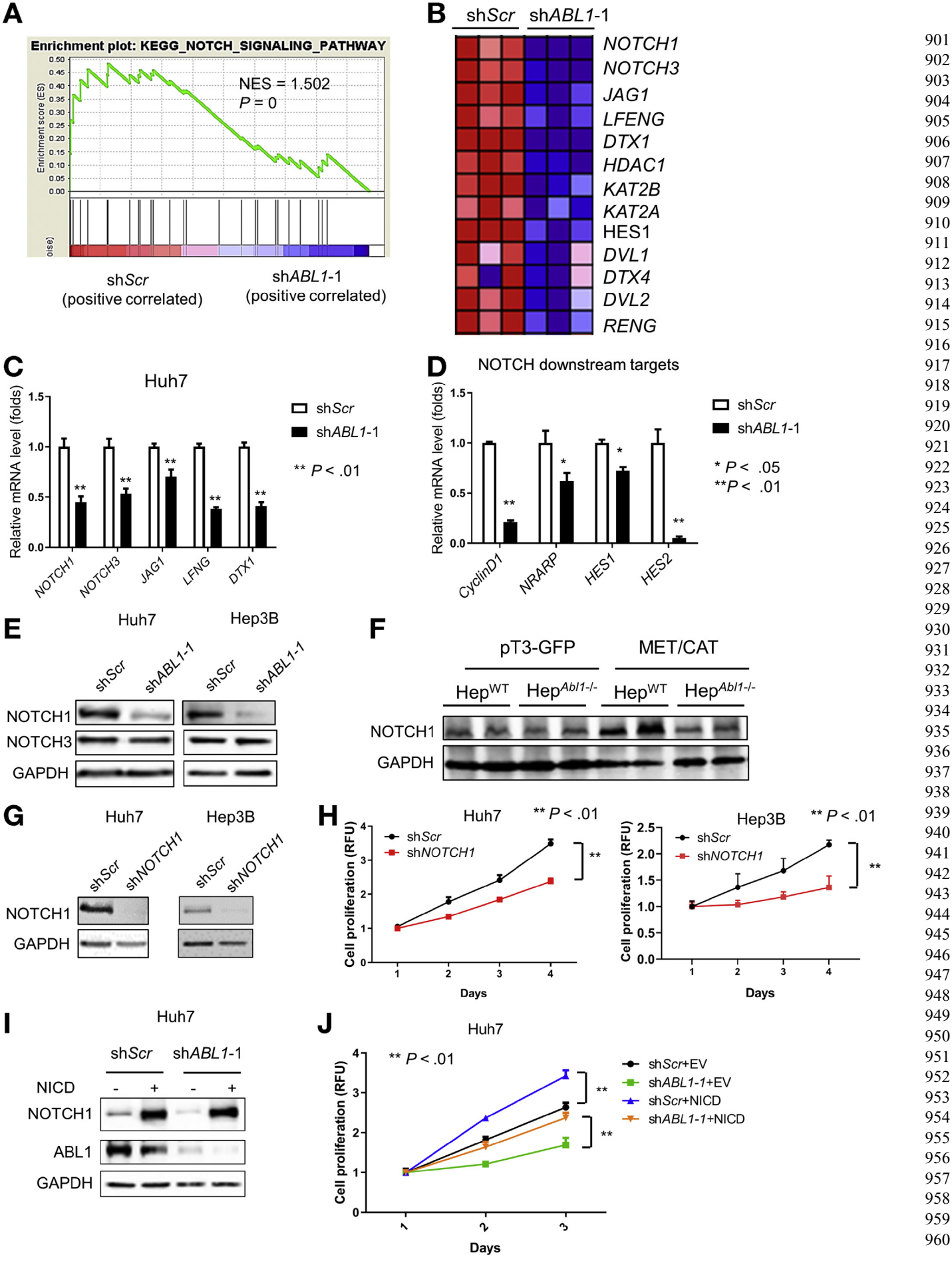

Knockdown of ABL1 *Inhibits Hepatocellular Carcinoma Cell Proliferation by Decreasing* NOTCH1 *Expression*

To determine the molecular mechanisms by which ABL1 promotes HCC cell proliferation, we performed RNA sequencing analysis using scrambled-control and ABL1-KD cells and proceeded to do GSEA. NOTCH signaling is one of the most significantly down-regulated gene pathways that result from ABL1 knockdown (Figure 4*A* and *B*). NOTCH signaling has been shown to play an important role in tumor cell growth in many types of cancer,[19] including HCC. We therefore hypothesized that knockdown of ABL1 inhibits HCC cell proliferation by inhibiting signaling along the NOTCH pathway. We used real-time polymerase chain reaction assays to confirm that ABL1 knockdown decreased mRNA expression for a number of NOTCH signaling pathway genes, including *NOTCH1*, *NOTCH3*, *JAG1*, *LFENG*, and *DTX1* (Figure 4*C*). We also found that expression of NOTCH downstream targets, including CyclinD1, NRARP, HES1, and HES2, were reduced by knockdown of ABL1 in HCC cells (Figure 4*D*), suggesting that NOTCH activity was suppressed in ABL1-KD cells.

Because NOTCH signaling receptors NOTCH1 and NOTCH3 play critical roles in HCC cell growth,[19–21] we focused on testing whether knockdown of ABL1 inhibits cell proliferation by decreasing the expression of either NOTCH1 or NOTCH3 in HCC cells. We first performed Western blotting to determine whether the expression of NOTCH1 and/or NOTCH3 proteins were also decreased by knockdown of ABL1 in HCC cells. Intriguingly, expression of NOTCH1 but not NOTCH3 protein was significantly lower in ABL1-KD cells compared to scrambled-RNA control cells (Figure 4*E*), suggesting a possible post-transcriptional, translational, or post-translational mechanism by which NOTCH3 might be regulated in ABL1-KD cells. We therefore focused on NOTCH1 and hypothesized that knockdown of ABL1 inhibits cell proliferation by decreasing NOTCH1 in HCC cells. We found that expression of NOTCH1 protein was higher in MET/CAT-induced liver tumors compared to control mouse liver, and was reduced in liver tumors when *Abl1* was deleted in hepatocytes (Figure 4*F*). Consistently, expression of NOTCH1-targeted genes was also down-regulated in *Abl1*-KO mouse HCCs (Supplementary Figure 6*A–C*). To further determine whether decreased NOTCH1 expression could inhibit HCC cell proliferation, we knocked down NOTCH1 using shRNA in Huh7 and Hep3B cells (Figure 4*G*). We tested 5 distinct shRNAs (data not shown) and only 1 shRNA efficiently decreased NOTCH1 expression in HCC cells (Figure 4*G*). We found that knockdown of NOTCH1 significantly reduced HCC cell growth (Figure 4*H*). In addition, NOTCH1 overexpression promoted cell proliferation and rescued the phenotype caused by ABL1 knockdown in HCC cells (Figure 4*I* and *J*). Overall, our data demonstrate that knockdown of ABL1 inhibits HCC cell growth by decreasing NOTCH1 expression.

Knockdown of ABL1 Decreases NOTCH1 Expression Through Regulation of c-MYC in Hepatocellular Carcinoma Cells

We next investigated the molecular mechanisms by which ABL1 knockdown decreases *NOTCH1* expression in HCC cells. As *NOTCH1* mRNA levels were reduced by ABL1 knockdown, we reasoned that this knockdown affected the transcription and/or post-transcriptional processing of *NOTCH1* mRNA. MicroRNAs (miRs) have been shown to directly target *NOTCH1* and reduce *NOTCH1* mRNA levels.[22] We therefore hypothesized that ABL1 knockdown might decrease *NOTCH1* expression by increasing the expression of some miR(s). Using TargetScan, we identified several miRs, including miR-150-5p, miR-34-5p, and miR-146b-5p, which can potentially directly target *NOTCH1*. However, we found that only the expression of miR-146b-5p was increased when ABL1 was knocked down in HCC cells (Supplementary Figure 7*A–C*). To determine whether ABL1 knockdown decreases *NOTCH1* expression through increasing miR-146b-5p expression in HCC cells, we used miR146b-5p mimics or inhibitors. We confirmed that the miR146b-5p mimic effectively induced expression of miR146b-5p and inhibitors of miR146b-5p sufficiently decreased expression of miR146b-5p (Supplementary Figure 7*D* and *E*). However, although we had expected that overexpression of miR146b-5p by the mimic miR would decrease expression of *NOTCH1* in HCC cells; instead we found that *NOTCH1* expression was slightly increased (Supplementary Figure 7*F*). Consistent with this observation, we found that miR146b-5p inhibition decreased the expression of *NOTCH1* in HCC cells (Supplementary Figure 7*G*). These data would appear to suggest that ABL1

Figure 4. ABL1 knockdown inhibits HCC cell proliferation by decreasing *NOTCH1* expression. (*A*) GSEA shows that the NOTCH signaling pathway is enriched in ABL1-KD Huh7 cells. (*B*) A heatmap indicates the expression of genes in the NOTCH signaling pathway is decreased by ABL1 knockdown in Huh7 cells. (*C*) Relative mRNA levels of genes in the NOTCH signaling pathway in scrambled-RNA and ABL1-KD Huh7 cells. (*D*) Relative mRNA levels of NOTCH downstream targets in the scrambled-RNA and ABL1-KD Huh7 cells. (*E*) NOTCH1, NOTCH3, and GAPDH protein expression in scrambled-RNA and ABL1-KD HCC cells was determined by Western blotting. (*F*) Expression of NOTCH1 and GAPDH proteins in whole livers of Hep^{WT} and $Hep^{Abl1-/-}$ mice injected with pT3-GFP or MET/CAT for 9 weeks was determined by Western blotting. (*G*) NOTCH1 and GAPDH protein expression in scrambled-RNA and NOTCH1-KD Hep3B and Huh7 cells was determined by Western blotting. (*H*) Quantification of cell proliferation from scrambled-RNA and NOTCH1-KD HCC cells at different time points after seeding. (*I*) Expression of NOTCH1, ABL1, and GAPDH proteins in control (infected with EF.CMV.GFP) and NOTCH1-overexpressed (infected with EF.hICN1.CMV.GFP) Huh7 scrambled and ABL1-KD cells was determined by Western blotting. (*J*) Quantification of cell proliferation from control and NOTCH1-overexpressed Huh7 scrambled and ABL1-KD cells at different time points after seeding.

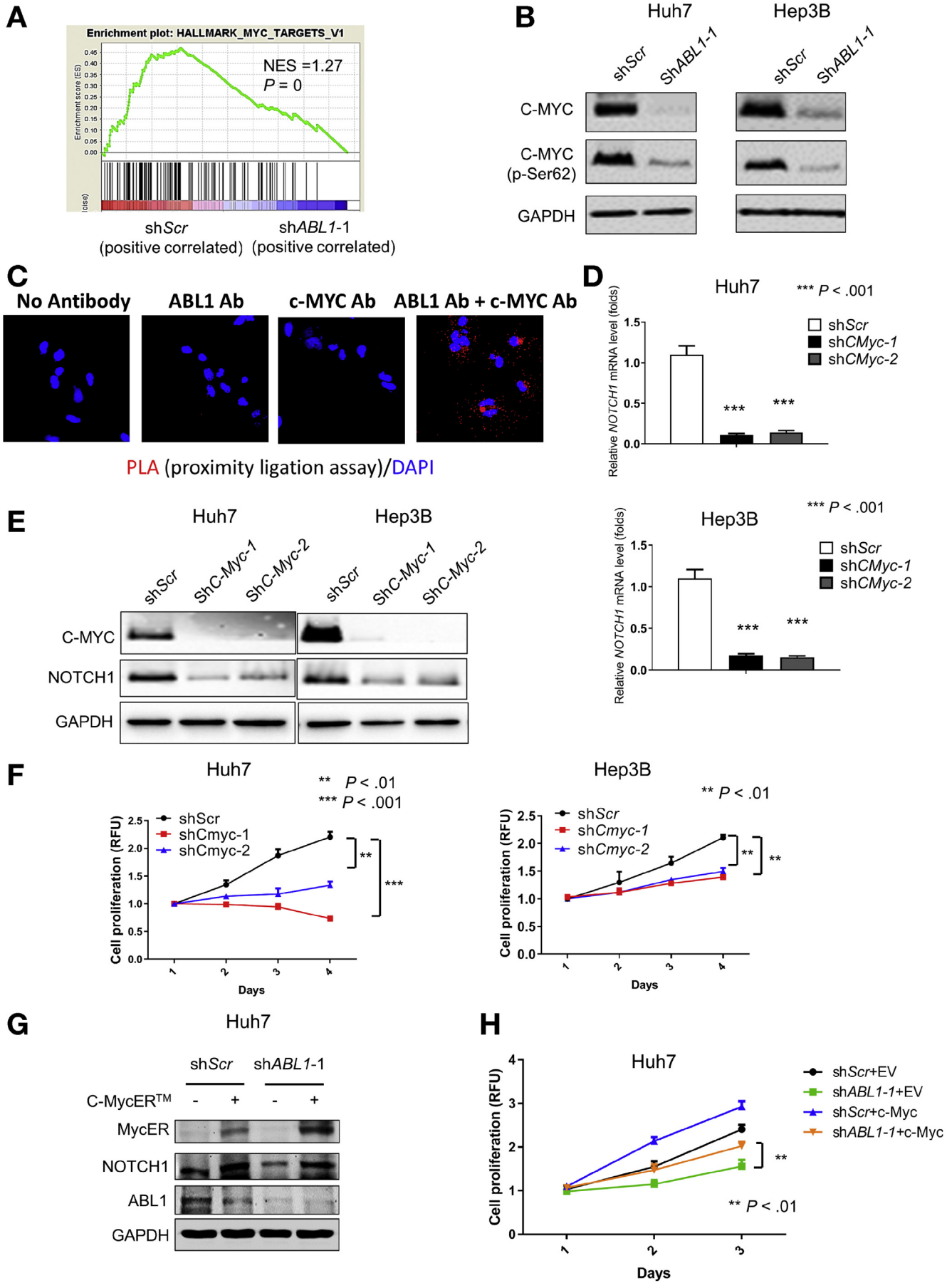

knockdown might not decrease *NOTCH1* expression by increasing the expression of miRs.

We therefore tested whether ABL1 knockdown reduces the transcription of *NOTCH1* by regulating transcription factors. ABL1 can regulate phosphorylation of the transcription factor c-MYC and its transcriptional activity.[23] c-MYC plays a critical role in HCC development.[24] Interestingly, GSEA indicated that MYC's target gene set was down-regulated in ABL1-KD cells (Figure 5*A*). Consistently, c-MYC protein level was much lower in ABL1-KD HCC cells compared to scrambled-RNA cells (Figure 5*B*). Expression of c-MYC protein was higher in MET/CAT-induced liver tumors compared to control mouse liver, and was reduced in liver tumors when *Abl1* was deleted in hepatocytes (Supplementary Figure 8). Phosphorylation of c-MYC on Ser62, which is regulated by ABL1[23] and is critical for c-MYC stabilization,[25] was also decreased by ABL1 knockdown (Figure 5*B*). In addition, using proximity ligation assay,[26] we found a strong interaction between ABL1 and c-MYC in HCC cells (Figure 5*C*, Supplementary Figure 9). Although c-*MYC* has been shown to be a direct transcriptional target downstream of NOTCH1 in T-cell acute lymphoblastic leukemia,[27] we found that c-MYC protein was not significantly affected by either knockdown or overexpression of NOTCH1 in HCC cells (Supplementary Figure 10). On the other hand, enhanced c-MYC expression may increase the level of *NOTCH1* mRNA through regulation of NRF2.[28,29] We therefore hypothesized that knockdown of ABL1 decreases *NOTCH1* expression through regulation of c-MYC in HCC cells. We found that both mRNA and protein expression of *NOTCH1* was decreased when c-MYC was knocked down in HCC cells (Figure 5*D* and *E*). In line with this, c-MYC knockdown inhibited HCC cell growth (Figure 5*F*). We analyzed the promoter of human *NOTCH1* and identified a putative binding site for c-MYC (Supplementary Figure 11*A*). The chromatin immunoprecipitation assay revealed that c-MYC directly binds to the promoter of *NOTCH1* in HCC cells (Supplementary Figure 11*B* and *C*). Moreover, overexpression of activated c-MYC promoted cell proliferation and restored decreased NOTCH1 expression and cell growth caused by ABL1 knockdown in HCC cells (Figure 5*G* and *H*). Considered altogether, these data indicate that knockdown of ABL1 decreases NOTCH1 expression through regulation of c-MYC in HCC cells.

Expression of p-ABL1, c-MYC, and NOTCH1 Is Positively Correlated in Human Hepatocellular Carcinoma

Our data indicate that ABL1 regulates the phosphorylation of c-MYC, leading to increased c-MYC protein levels, which results in enhanced *NOTCH1* mRNA expression and promotes HCC cell growth (Figure 6*A*). To determine whether the ABL1/c-MYC/NOTCH1 axis is also relevant in human HCC, we examined the levels of p-ABL1 (Y412) (an indicator of ABL1 activity), c-MYC, and NOTCH1 in human HCC specimens using tissue microarrays. The expression of both c-MYC and NOTCH1 proteins was significantly correlated with levels of p-ABL1 in human HCC specimens (Figure 6*B–D*). In addition, NOTCH1 protein expression correlated with c-MYC in human HCC (Figure 6*E*). We further analyzed the TCGA database and found that *NOTCH1* mRNA level positively correlated with *ABL1* mRNA level (Figure 6*F*). However, *c-MYC* mRNA level had no correlation with either *ABL1* or *NOTCH1* mRNA level in the TCGA HCC samples (Supplementary Figure 12), suggesting that ABL1 may not regulate c-MYC at transcript level in human HCC. Overall, these data indicate that the ABL1/c-MYC/NOTCH1 axis is important in human HCC.

ABL1 Inhibitors Suppress Hepatocellular Carcinoma Growth in Preclinical Models

The above results encouraged us to examine whether ABL1 inhibitors could be useful to treat HCC in preclinical models, which would provide a translational basis for the potential clinical use of ABL1 inhibitors in the treatment of HCC patients. Several ABL kinase inhibitors are already used clinically or are under investigation in clinical trials for treating chronic myelogenous leukemia and other cancers,4 but their efficacy in HCC remains unknown. Nilotinib, an ATP-competitive inhibitor of ABL kinases, has been approved by the US Food and Drug Administration to treat Philadelphia chromosome–positive chronic myelogenous leukemia.[30] GNF-5, a newer allosteric inhibitor that targets the myristate pocket of ABL kinases, has been tested in preclinical leukemia models.[31] Because ABL1 knockdown inhibits HCC cell growth (Figure 3), we

Figure 5. Knockdown of ABL1 decreases NOTCH1 expression through regulation of c-MYC in HCC cells. (*A*) GSEA shows that the MYC targets are enriched in ABL1-KD Huh7 cells. (*B*) Levels of c-MYC, p-c-MYC (Ser62), and GAPDH proteins in scrambled-RNA and ABL1-KD HCC cells was determined by Western blotting. (*C*) The interaction of ABL1 and c-MYC was examined using proximity ligation assay in Huh7 cells. (*D*) Relative mRNA levels of *NOTCH1* in scrambled-RNA control and c-MYC-KD HCC cells. (*E*) Expression of c-MYC, NOTCH1, and GAPDH proteins in scrambled-RNA and c-MYC-KD HCC cells was determined by Western blotting. (*F*) Quantification of cell proliferation from scrambled-RNA and c-MYC-KD HCC cells. (*G*) Expression of MycER (activated fusion c-MYC), NOTCH1, ABL1, and GAPDH proteins in control (infected with the pBpuro retroviral particle) and c-MYC–overexpressed (infected with the pBpuro c-MYCER retroviral particle) Huh7 scrambled and ABL1-KD cells was determined by Western blotting. (*H*) Quantification of cell proliferation from in control and c-MYC-overexpressed Huh7 scrambled and ABL1-KD cells.

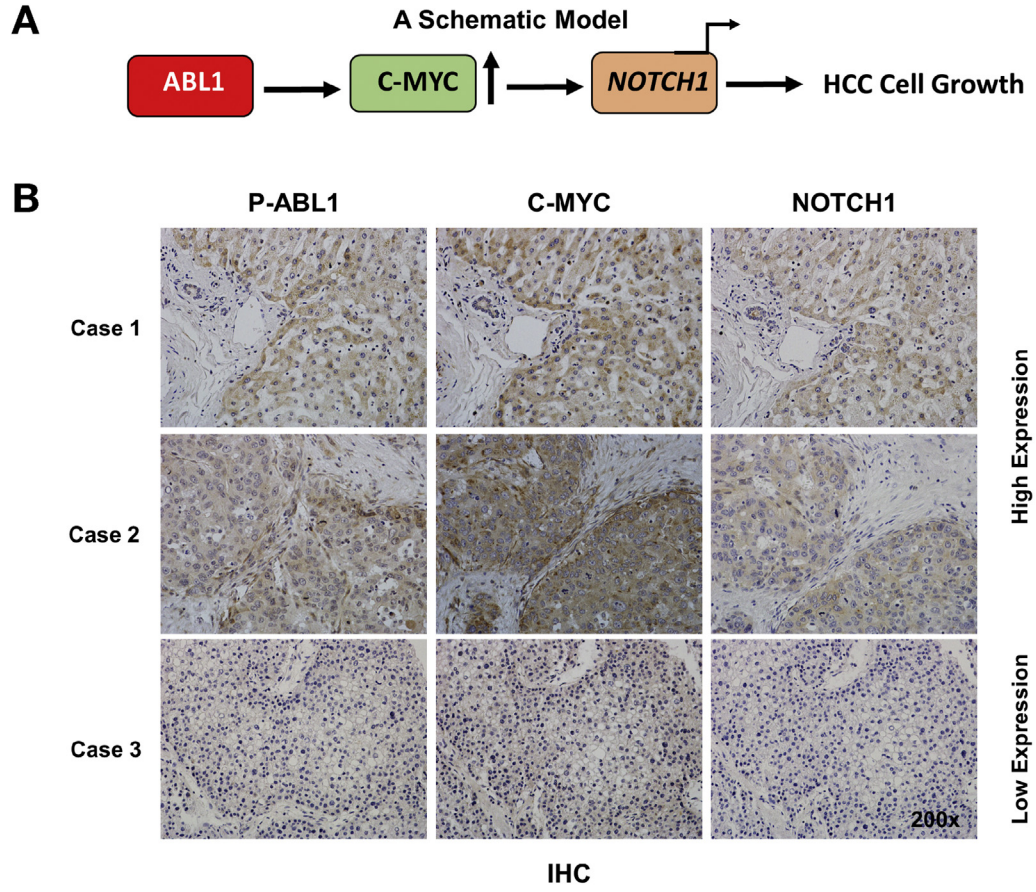

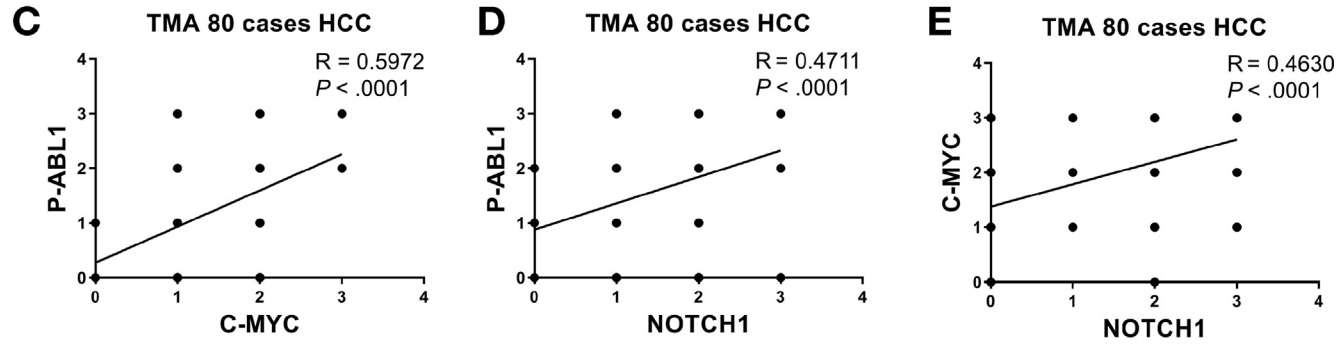

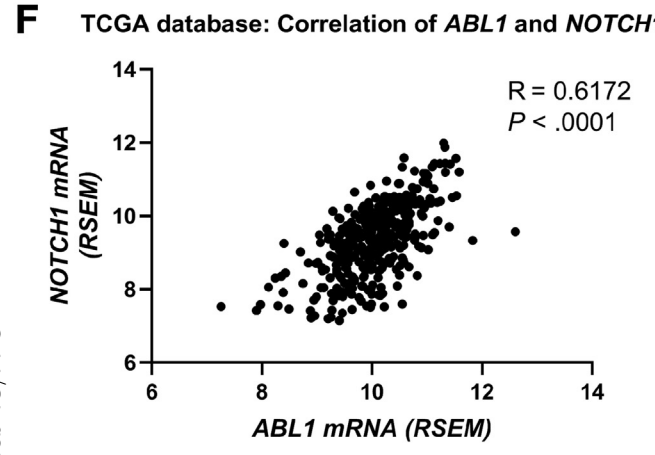

hypothesized that ABL inhibitors would be efficacious in treating HCC. First, we confirmed that both nilotinib and GNF-5 effectively inhibit ABL kinase activity, as indicated by phosphorylation of CRKL in HCC cells (Supplementary Figure 13*A* and *B*). Further, we found that both nilotinib and GNF5 inhibited HCC cell growth in vitro (Figure 7*A*, Supplementary Figures 13*C* and 14*A*). Importantly, the sensitivity of nilotinib positively correlated with the expression of ABL1 (Figure 7*B* and Supplementary Figure 14*B*). We also found there is a positive correlation between ABL1 and c-MYC expression in human HCC cell lines (Supplementary Figure 14*B* and *C*). However, there is no significant correlation between ABL1 and NOTCH1 in these HCC cell lines (Supplementary Figure 14*B* and *C*), suggesting other mechanisms may also regulate NOTCH1 expression. It is notable that NOTCH1 expression is positively correlated with ABL1 in HCC cells without p53 mutations (Hep3B, Huh7, SK-Hep1 and SNU-423), but there is no correlation in p53-mutant HCC cells (SNU-449, SNU-475, PLC/PRF/5, and SNU-387), suggesting that p53 mutations may affect NOTCH1 expression. Consistent with the functional inhibition of ABL1 using shRNAs, nilotinib effectively decreased the expression of c-MYC and NOTCH1 (Figure 7*C*). Moreover, nilotinib significantly suppressed tumor growth (Figure 7*D*–*G*) and proliferation (Supplementary Figure 15*A*–*D*) in an HCC xenograft model. To further test the efficacy of ABL inhibitors in mouse models with intact immune responses, we injected wild-type C57BL/6 mice with MET/CAT to induce HCC and gavaged these mice with nilotinib or vehicle solution by oral gavage daily for 4 weeks. We found that nilotinib treatment dramatically inhibited MET/CAT-induced tumor growth (Figure 7*H* and *I*) and proliferation (Supplementary Figure 16), decreased the expression of MYC and NOTCH1 (Figure 7*J*), and prolonged the survival of animals with HCC (Figure 7*K*). In contrast, sorafenib was not effective in inhibiting MET/CAT-induced HCC growth (Supplementary Figure 17). Taken together, these data indicate that ABL1 inhibitors effectively suppress HCC growth in preclinical models.

Discussion

Tyrosine kinases have been shown to be good targets for treating cancer, including HCC. Currently, 4 of every 5 drugs approved to treat advanced HCC are tyrosine kinase inhibitors.[2] Despite the success of tyrosine kinase inhibitors in treating HCC, many patients do not respond. There is significant genetic and biological heterogeneity in HCC. A better understanding of tyrosine kinases in the development HCC is necessary in order to predict response to therapy and to develop new therapies. Only a few tyrosine kinases have been shown to play key roles in HCC initiation and progression.[32] In this study, we found that ABL1 is overexpressed and activated in human HCCs, and ABL1 inhibition effectively suppresses HCC growth in human and mouse preclinical models, suggesting that inhibition of ABL1 may be a promising new strategy to treat HCC. We showed that ABL1 inhibitors such as nilotinib significantly inhibit HCC growth in vitro and in vivo. Our findings provide translational support for the development of a clinical trial to assess the safety and efficacy of nilotinib in treating HCC.

How ABL1 is activated in HCC remains unclear. MET can bind directly to ABL1 and activate it in breast cancer cells.[16] We found that ABL1 is activated in MET/CAT-induced HCC tumors, suggesting that ABL1 might be activated by MET in human HCC. In addition, we found that ABL1 expression was also increased in MET/CAT-induced liver tumors. Consistently, *ABL1* mRNA expression is highly correlated with the gene signature of activated MET in human HCC (Supplementary Figure 18).[17] Therefore, it is possible that *ABL1* mRNA expression can be up-regulated by activated MET in HCC. SP1 can modulate ABL1 expression at the transcription level,[33] and MET can induce the phosphorylation of SP1 and enhance its transcriptional activity.[34] Thus, MET activation may increase *ABL1* mRNA expression through the regulation of SP1. This hypothesis will be tested in our future studies.

For the first time, we demonstrated that the NOTCH signaling pathway is suppressed by ABL1 knockdown in HCC cells. NOTCH signaling is a crucial determinant of tumor cell growth in many types of cancer, including HCC.[19] However, NOTCH inhibitors such as GSI cause gastrointestinal toxicity due to its off-target effects.[35] Our data suggest a possible new strategy to inhibit the NOTCH pathway, which would be to inhibit ABL1. As functional inhibition of ABL1 showed low and tolerable toxicity, ABL1 inhibitors might be useful to treat HCC cases that exhibit up-regulated NOTCH signaling. It remains to be determined whether the regulation of the NOTCH signaling pathway by ABL1 is tissue- or cell-context–dependent. Our findings might provide a broader application for using ABL1 inhibitors in other type of cancers with activated NOTCH. For example, NOTCH signaling is known to play a critical role in intrahepatic cholangiocarcinoma.[36] Currently, there are no targeted therapy options available for intrahepatic cholangiocarcinoma. It would be intriguing

Figure 6. Levels of p-ABL1, c-MYC or NOTCH1 are positively correlated in human HCC. (*A*) A schematic model: ABL1 activation (due to ABL1 overexpression or other reasons) leads to an increase of c-MYC protein expression and its transcriptional activity with respect to *NOTCH1*, thereby promoting HCC cell proliferation. (*B*) Levels of p-ABL1 (p-Y412), c-MYC, and NOTCH1 in human HCC specimens (tissue microarrays) were determined by IHC staining. (*C*) Correlation of p-ABL1 and c-MYC levels in human HCC specimens was analyzed. (*D*) Correlation of p-ABL1 and NOTCH1 levels in human HCC specimens was analyzed. (*E*) Correlation of c-MYC and NOTCH1 expression in human HCC specimens was analyzed. (*F*) Correlation of *ABL1* and *NOTCH1* mRNAs in HCC samples from the TCGA database was analyzed.

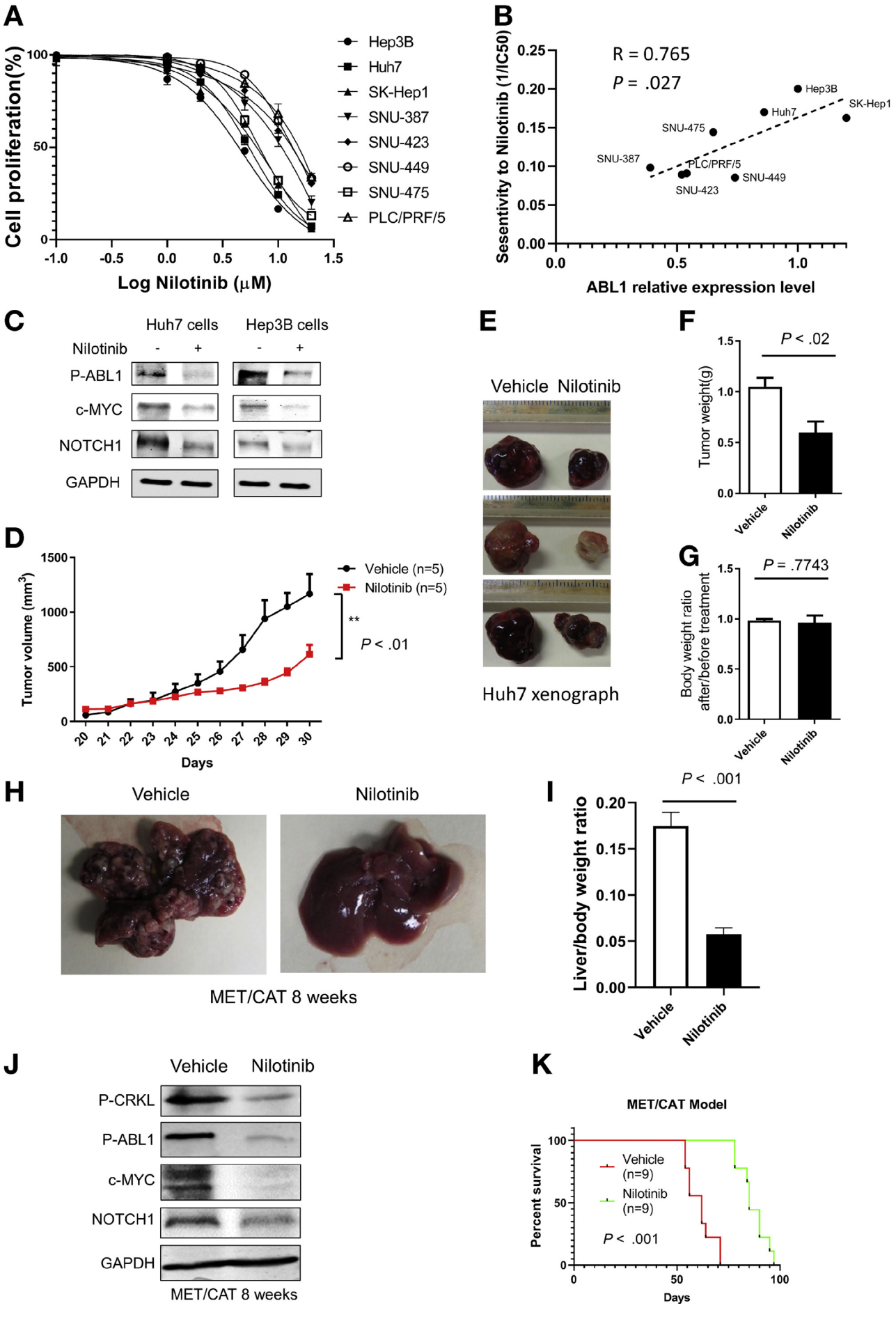
A
Cell proliferation(%)
Log Nilotinib (μM)
Hep3B
Huh7
SK-Hep1
SNU-387
SNU-423
SNU-449
SNU-475
PLC/PRF/5
B
Sesentivity to Nilotinib (1/IC50)
ABL1 relative expression level
R = 0.765
P = .027
C
Huh7 cells
Hep3B cells
Nilotinib
P-ABL1
c-MYC
NOTCH1
GAPDH
D
Tumor volume (mm3)
Days
Vehicle (n=5)
Nilotinib (n=5)
P < .01
E
Vehicle Nilotinib
Huh7 xenograph
F
Tumor weight(g)
P < .02
G
Body weight ratio after/before treatment
P = .7743
H
Vehicle
Nilotinib
MET/CAT 8 weeks
I
Liver/body weight ratio
P < .001
J
Vehicle Nilotinib
P-CRKL
P-ABL1
c-MYC
NOTCH1
GAPDH
MET/CAT 8 weeks
K
MET/CAT Model
Percent survival
Vehicle (n=9)
Nilotinib (n=9)
P < .001
Days

to test whether ABL1 inhibitors might be useful in inhibiting intrahepatic cholangiocarcinoma growth in future studies.

ABL kinases function by regulating more than 100 different targets in a cell-context–specific manner, making it difficult to select appropriate downstream targets of ABL1 for study.[4] ABL1 has been reported to phosphorylate AKT and ERK to regulate cancer cell proliferation and survival.[37] However, ABL1 knockdown did not affect phosphorylation of either AKT or ERK in HCC cells (Supplementary Figure 19), which supports the concept that ABL1's regulation of different targets is cell-context–dependent. We found that ABL1 knockdown decreases c-MYC protein expression and further demonstrated that decreased c-MYC results in reduced NOTCH1 expression in HCC cells. These data reveal a novel mechanism by which ABL1 promotes cell growth in HCC. c-MYC is a well-known proto-oncogene that plays a critical role in many cancers, including liver cancer.[38] However, it is still currently "untargetable" clinically. Our results suggest that inhibition of ABL1 might be useful to treat HCC cases demonstrating high expression of c-MYC. Although c-MYC is a direct transcriptional target downstream of NOTCH1 in T-ALL,[27] our data suggest that c-MYC may not be regulated by NOTCH1 in HCC cells. This is not particularly surprising, as NOTCH1 regulates different targets in tissue- and cell-context–dependent manners.[39] It remains unknown whether c-MYC regulates NOTCH1 in other contexts, as this mechanism has not been reported previously. It will be instructive to examine whether this regulation occurs in other cancers. Besides the c-MYC/NOTCH1 axis, we also identified other signaling pathways regulated by ABL1 in HCC cells through RNA sequencing analysis. The gene sets that are most significantly downregulated by ABL1 knockdown include hypoxia, the p53 pathway, glycolysis, and androgen response (Supplementary Figure 20), which have been shown to regulate tumor growth and progression.[40–43] It is possible that ABL1 promotes HCC development through regulation of these signaling pathways, and we plan to investigate this in our future studies.

In conclusion, our study shows that ABL1 plays a critical role in the development of HCC by regulating the c-MYC/NOTCH1 axis. Inhibition of ABL1 represents a promising new strategy to treat HCC in patients who overexpress this protein-tyrosine kinase. A number of ABL kinase inhibitors have been developed and are being used clinically for leukemia and gastrointestinal stromal tumors. These inhibitors might also prove to be useful in treating HCC, especially in patients showing overexpression and/or activation of ABL1.

Supplementary Material

Note: To access the supplementary material accompanying this article, visit the online version of *Gastroenterology* at www.gastrojournal.org, and at http://dxdoi.org/10.1053/j.gastro.2020.03.013.

References

1. Bray F, Ferlay J, Soerjomataram I, et al. Global cancer statistics 2018: GLOBOCAN estimates of incidence and mortality worldwide for 36 cancers in 185 countries. CA Cancer J Clin 2018;68:394–424.
2. Heimbach JK, Kulik LM, Finn RS, et al. AASLD guidelines for the treatment of hepatocellular carcinoma. Hepatology 2018;67:358–380.
3. Marrero JA, Kulik LM, Sirlin CB, et al. Diagnosis, staging, and management of hepatocellular carcinoma: 2018 practice guidance by the American Association for the Study of Liver Diseases. Hepatology 2018;68:723–750.
4. Greuber EK, Smith-Pearson P, Wang J, et al. Role of ABL family kinases in cancer: from leukaemia to solid tumours. Nat Rev Cancer 2013;13:559–571.
5. Chitsike L, Ding X, Breslin P, et al. ABL1 is overexpressed and activated in hepatocellular carcinoma. J Cancer Tumor Int 2017;6:8.
6. Wang F, Bank T, Malnassy G, et al. Inhibition of insulin-like growth factor 1 receptor enhances the efficacy of sorafenib in inhibiting hepatocellular carcinoma cell growth and survival. Hepatol Commun 2018;2:732–746.
7. Arteaga M, Shang N, Ding X, et al. Inhibition of SIRT2 suppresses hepatic fibrosis. Am J Physiol Gastrointest Liver Physiol 2016;310:G1155–G1168.
8. Littlewood TD, Hancock DC, Danielian PS, et al. A modified oestrogen receptor ligand-binding domain as an improved switch for the regulation of heterologous proteins. Nucleic Acids Res 1995;23:1686–1690.
9. Vichai V, Kirtikara K. Sulforhodamine B colorimetric assay for cytotoxicity screening. Nat Protoc 2006;1:1112–1116.
10. Shang N, Arteaga M, Zaidi A, et al. FAK is required for c-Met/beta-catenin-driven hepatocarcinogenesis. Hepatology 2015;61:214–226.

Figure 7. ABL1 inhibitors suppress human HCC growth in vitro and in vivo. (*A*) Quantification of cell proliferation of HCC cells treated with vehicle or nilotinib at different dose after 48 hours treatment. (*B*) Correlation between ABL1 expression and sensitivity to nilotinib in HCC cells described in (*A*). (*C*) Levels of p-ABL, c-MYC, NOTCH1, and GAPDH proteins in HCC cells treated with vehicle or 5 μM nilotinib for 24 hours. (*D*) SCID-bg mice injected with Huh7 cells were gavaged with vehicle or nilotinib for 10 days and tumor volumes from mice (n = 5/group) were measured. (*E*) *Gross images* of tumors from vehicle- or nilotinib-gavaged animals are shown. (*F*) Tumor weights from mice from (*D*). (*G*) Body weight ratios from mice after/before nilotinib treatment. (*H*) C57BL/6 mice were injected with MET/CAT to induce HCC. Four weeks after such injection, the mice were gavaged with vehicle or nilotinib for 4 weeks (some mice treated with vehicle had to be euthanized earlier due to tumor burdens), and *gross images* of livers from vehicle- and nilotinib-gavaged animals at 8 weeks after MET/CAT injection are shown. (*I*) Liver/body weight ratios from the mice (n = 6/group). (*J*) Levels of p-CRKL, p-ABL, c-MYC, NOTCH1, and GAPDH proteins in the mouse livers from (*H*). (*K*) Survival graphs for mice gavaged with vehicle or nilotinib (n = 9/group).

11. **Shang N, Wang H,**Bank T, et alFocal adhesion kinase and beta-catenin cooperate to induce hepatocellular carcinomaHepatology 2019;70:1631–1645.
12. Cancer Genome Atlas Research Network. Electronic address: wheeler@bcm.edu; Cancer Genome Atlas Research Network. Comprehensive and integrative genomic characterization of hepatocellular carcinoma. Cell 2017;169:1327–1341.e23.
13. Van Etten RA. Cycling, stressed-out and nervous: cellular functions of c-Abl. Trends Cell Biol 1999;9:179–186.
14. Dorey K, Engen JR, Kretzschmar J, et al. Phosphorylation and structure-based functional studies reveal a positive and a negative role for the activation loop of the c-Abl tyrosine kinase. Oncogene 2001;20:8075–8084.
15. Brasher BB, Van Etten RA. c-Abl has high intrinsic tyrosine kinase activity that is stimulated by mutation of the Src homology 3 domain and by autophosphorylation at two distinct regulatory tyrosines. J Biol Chem 2000; 275:35631–35637.
16. Li R, Knight JF, Park M, et al. Abl kinases regulate HGF/Met signaling required for epithelial cell scattering, tubulogenesis and motility. PLoS One 2015;10: e0124960.
17. Tao J, Xu E, Zhao Y, et al. Modeling a human hepatocellular carcinoma subset in mice through coexpression of met and point-mutant beta-catenin. Hepatology 2016; 64:1587–1605.
18. de Jong R, ten Hoeve J, Heisterkamp N, et al. Tyrosine 207 in CRKL is the BCR/ABL phosphorylation site. Oncogene 1997;14:507–513.
19. Yuan X, Wu H, Xu H, et al. Notch signaling: an emerging therapeutic target for cancer treatment. Cancer Lett 2015;369:20–27.
20. Wu CX, Xu A, Zhang CC, et al. Notch inhibitor PF-03084014 inhibits hepatocellular carcinoma growth and metastasis via suppression of cancer stemness due to reduced activation of Notch1-Stat3. Mol Cancer Ther 2017;16:1531–1543.
21. Zhou L, Zhang N, Song W, et al. The significance of Notch1 compared with Notch3 in high metastasis and poor overall survival in hepatocellular carcinoma. PLoS One 2013;8:e57382.
22. Mei J, Bachoo R, Zhang CL. MicroRNA-146a inhibits glioma development by targeting Notch1. Mol Cell Biol 2011;31:3584–3592.
23. Sanchez-Arevalo Lobo VJ, Doni M, Verrecchia A, et al. Dual regulation of Myc by Abl. Oncogene 2013;32:5261–5271.
24. Dang H, Takai A, Forgues M, et al. Oncogenic activation of the RNA binding protein NELFE and MYC signaling in hepatocellular carcinoma. Cancer Cell 2017;32:101–114.e8.
25. Sears R, Nuckolls F, Haura E, et al. Multiple Ras-dependent phosphorylation pathways regulate Myc protein stability. Genes Dev 2000;14:2501–2514.
26. Soderberg O, Gullberg M, Jarvius M, et al. Direct observation of individual endogenous protein complexes in situ by proximity ligation. Nat Methods 2006;3:995–1000.
27. Palomero T, Lim WK, Odom DT, et al. NOTCH1 directly regulates c-MYC and activates a feed-forward-loop transcriptional network promoting leukemic cell growth. Proc Natl Acad Sci U S A 2006;103:18261–18266.
28. DeNicola GM, Karreth FA, Humpton TJ, et al. Oncogene-induced Nrf2 transcription promotes ROS detoxification and tumorigenesis. Nature 2011;475:106–109.
29. Wakabayashi N, Shin S, Slocum SL, et al. Regulation of notch1 signaling by nrf2: implications for tissue regeneration. Sci Signal 2010;3:ra52.
30. Weisberg E, Catley L, Wright RD, et al. Beneficial effects of combining nilotinib and imatinib in preclinical models of BCR-ABL+ leukemias. Blood 2007;109:2112–2120.
31. **Zhang J, Adrian FJ,**Jahnke W, et alTargeting Bcr-Abl by combining allosteric with ATP-binding-site inhibitorsNature 2010;463:501–506.
32. Regad T. Targeting RTK signaling pathways in cancer. Cancers (Basel) 2015;7:1758–1784.
33. Long J, Liao G, Wang Y, et al. Specific protein 1, c-Abl and ERK1/2 form a regulatory loop. J Cell Sci 2019; 132:jcs222380.
34. Reisinger K, Kaufmann R, Gille J. Increased Sp1 phosphorylation as a mechanism of hepatocyte growth factor (HGF/SF)-induced vascular endothelial growth factor (VEGF/VPF) transcription. J Cell Sci 2003;116:225–238.
35. Venkatesh V, Nataraj R, Thangaraj GS, et al. Targeting Notch signalling pathway of cancer stem cells. Stem Cell Invest 2018;5:5.
36. Geisler F, Strazzabosco M. Emerging roles of Notch signaling in liver disease. Hepatology 2015;61:382–392.
37. Hantschel O. Structure, regulation, signaling, and targeting of abl kinases in cancer. Genes Cancer 2012; 3:436–446.
38. Gabay M, Li Y, Felsher DW. MYC activation is a hallmark of cancer initiation and maintenance. Cold Spring Harb Perspect Med 2014;4.
39. Andersson ER, Sandberg R, Lendahl U. Notch signaling: simplicity in design, versatility in function. Development 2011;138:3593–3612.
40. Nath B, Szabo G. Hypoxia and hypoxia inducible factors: diverse roles in liver diseases. Hepatology 2012;55:622–633.
41. Meng X, Franklin DA, Dong J, et al. MDM2-p53 pathway in hepatocellular carcinoma. Cancer Res 2014;74:7161–7167.
42. Alves AP, Mamede AC, Alves MG, et al. Glycolysis inhibition as a strategy for hepatocellular carcinoma treatment? Curr Cancer Drug Targets 2019; 19:26–40.
43. Ma WL, Lai HC, Yeh S, et al. Androgen receptor roles in hepatocellular carcinoma, fatty liver, cirrhosis and hepatitis. Endocr Relat Cancer 2014;21:R165–R182.

Author names in bold designate shared co-first authorship.

Received July 9, 2019. Accepted March 4, 2020.

Correspondence
Address correspondence to: Wei Qiu, PhD, Departments of Surgery and Cancer Biology, Loyola University Chicago Stritch School of Medicine, 2160 South 1st Avenue, Maywood, Illinois 60153. e-mail: wqiu@luc.edu; fax: 708-327-3342. Q4

Acknowledgments
The authors thank Drs Clodia Osipo, Nancy Zeleznik-Le, and Jiwang Zhang of Loyola University Chicago and Dr Ann Marie Pendergast of Duke University for their helpful discussions and advice.

CRediT Authorship Contributions
Fang Wang, PhD (Data curation: Equal; Formal analysis: Equal; Investigation: Equal; Methodology: Lead; Writing – original draft: Lead; Writing – review & editing: Supplementary). Wei Hou, MD/PhD (Data curation: Equal; Formal analysis: Equal; Investigation: Equal; Methodology: Equal; Writing – review & editing: Supplementary). Lennox Chitsike, MS (Data curation: Supplementary; Formal analysis: Supplementary; Investigation: Supplementary; Methodology: Supplementary). Yingchen Xu, MD, PhD (Data curation: Supplementary; Investigation: Supplementary). Carlee Bettler, BS (Formal analysis: Supplementary; Methodology: Supplementary). Thomas Bank, BS (Data curation: Supplementary; Investigation: Supplementary). Aldeb Perera, BS (Data curation: Supplementary; Investigation: Supplementary). Scott J. Cotler, MD (Conceptualization: Supplementary; Writing – original draft: Supplementary; Writing – review & editing: Supplementary). Asha Dhanarajan, MD (Conceptualization: Supplementary; Writing – original draft: Supplementary; Writing – review & editing: Supplementary). Mitchell F Denning, PhD (Investigation: Supplementary; Methodology: Supplementary; Writing – review & editing: Supplementary). Xianzhong Ding, MD, PhD (Formal analysis: Supplementary; Investigation: Supplementary; Methodology: Supplementary; Visualization: Supplementary). Peter Breslin, PhD (Writing – original draft: Supplementary; Writing – review & editing: Supplementary). Wenan Qiang, PhD (Investigation: Supplementary). Jun Li, PhD (Formal analysis: Equal; Investigation: Supplementary). Anthony J. Koleske, PhD (Conceptualization: Supplementary; Funding acquisition: Supplementary; Investigation: Supplementary; Writing – original draft: Supplementary; Writing – review & editing: Supplementary). Wei Qiu, PhD (Conceptualization: Lead; Formal analysis: Supplementary; Funding acquisition: Lead; Project administration: Lead; Writing – original draft: Lead; Writing – review & editing: Lead).

Conflicts of interest
The authors disclose no conflicts. Q5

Funding
This work was supported in part by ACS RSG-18-107 (W. Qiu), NIH R01NS105640 (A. Koleske), NIH R01MH115939 (A. Koleske), NIH R03CA195183 (W. Qiu), R03CA184652 (W. Qiu), and R01CA197128 (W. Qiu). Q6 Q16

Supplementary Experimental Procedures

Cells and Reagents

Huh7, Hep3B, PLC/PRF/5, Skep-1, and 293T cells were cultured in Dulbecco's modified Eagle's medium (high-glucose; Thermo Scientific, Waltham, MA), supplemented with 10% fetal bovine serum (Tissue Culture Biologicals, Tulare, CA), penicillin, and streptomycin (Sigma-Aldrich) in a humidified atmosphere of 5% CO_2 at 37°C. SNU387, SNU423, SNU449, and SNU475 were cultured in RPMI-1640 medium supplemented with 10% fetal bovine serum (Tissue Culture Biologicals) and 1× penicillin/streptomycin (Sigma-Aldrich) at 37°C and 5% CO_2.

The Cancer Genome Atlas Data Analysis

The data for all boxplots and correlation plots were retrieved from the UCSC Xena platform (https://xenabrowser.net/), specifically from the TCGA Liver Cancer (LIHC) study. For the first variable, the data type selected was "Genomic" and the assay type selected was "Gene Expression." For the second variable, the data type selected was "Phenotypic." To create the boxplots in R software, version 3.6.0, gene expression values were first separated into the categories "normal tissue," consisting of solid tissue normal samples, and "tumor tissue," consisting of primary tumor and recurrent tumor samples. These sorted data were then plotted using the function boxplot. *P* values were generated using Welch's *t* test on 2-sample, unpaired data. Normality required for all *t* tests was assumed by central limit theorem and visual inspection of boxplots. The correlation plots were created using GraphPad Prism software, version 8.0.1. The Pearson's coefficient of correlation, *R*, and its respective *P* value (2-tailed) were also calculated using GraphPad Prism software, version 8.0.1.

The data for Kaplan-Meier plots were retrieved from the pathology atlas section of the Human Protein Atlas (https://www.proteinatlas.org/humanproteome/pathology). Liver cancer TCGA RNA sample, description, and FPKM data were used for each individual gene. To create the Kaplan-Meier plots, Python software, version 3.0 was used to modify the original data from the Pathology Atlas. Specifically, censored data were generated by dividing patients into 2 groups in which the censored group consisted of patients who had not died by the end of the study time. Patient data were also separated into 2 different groups based on the expression level indicated by FKPM values, for which the dividing threshold was provided by the Pathology Atlas. Binary censored data, binary expression group data, and survival times were imported into R software, version 3.6.0, where Kaplan-Meier plots were created using the survival, survminer, dplyr packages and the Surv, survfit, and ggsurvplot functions. *P* values were generated by including the command "pval = TRUE" in the ggsurvplot function from the survminer library. Based on the FPKM value of each gene, patients were classified into 2 groups and association between prognosis (survival) and gene expression (FPKM) was examined. The best expression cutoff refers the FPKM value that yields maximal difference with regard to survival between the 2 groups at the lowest log-rank *P* value. Best expression cutoff was selected based on survival analysis. If FPKM values were greater than or equal to the best expression cutoff value, they were defined as high. If they were lower than this they were defined as low. We also used the median (50%) group cutoff method and found similar results.

MET/CAT-Induced Hepatocellular Carcinoma Model

For the MET/CAT-driven HCC model, 50 μg of total plasmids, encoding the Sleeping Beauty transposase (HSB2) and transposons with GFP (pT3-GFP) or MET gene and catenin β1 gene with the N-terminal truncation (referred to here as MET/CAT) (22.5 μg pT3-EF1a-MET, 22.5 μg pT3-EF1a-ΔN90-β-catenin, and 5 μg HSB2) were injected hydrodynamically into age- and sex-matched mice as described previously.[1,2] All mice were maintained on the standard diet until being euthanized.

Proximity Ligation Assay

Proximity ligation assay was performed using the Duolink In Situ Red Starter Kit Mouse/Rabbit (MilliporeSigma) according to the manufacturer's instructions. In brief, cells were seeded onto an 8-well-Nunc Lab-Tek II CC2 Chamber Slide System (Thermo Fisher) at 17.5 × 10^3/well overnight, then fixed with 4% paraformaldehyde for 30 minutes at room temperature and washed in phosphate-buffered saline, followed by permeabilization with 0.1% Triton X-100 for 10 minutes. After washing with Wash Buffer A (MilliporeSigma) followed by blocking with Duolink Blocking Buffer (MilliporeSigma) for 30 minutes at room temperature, cells were incubated with primary antibodies (ABL1, #2862, 1:100; Cell Signaling and c-MYC, #5605, 1:100; Cell Signaling) overnight at 4°C. The following day, cells were washed repeatedly in Wash Buffer A, followed by incubation with appropriate Duolink secondary antibodies (MilliporeSigma) for 1 hour at 37°C. According to the manufacturer's protocol. After washing with Wash Buffer A at room temperature, ligation, and amplification steps of the proximity ligation assay were performed according to the manufacturer's protocol. After final washes with Wash Buffer B at room temperature, slides were mounted with Corning 24 × 50 mm Rectangular #1 Cover Glass (Corning, Corning, NY) using Duolink In Situ Mounting Medium with 4′,6-diamidino-2-phenylindole (MilliporeSigma).

Supplementary References

1. Patil MA, Lee SA, Macias E, et al. Role of cyclin D1 as a mediator of c-Met- and beta-catenin-induced hepatocarcinogenesis. Cancer Res 2009;69:253–261.
2. Shang N, Arteaga M, Zaidi A, et al. FAK is required for c-Met/beta-catenin-driven hepatocarcinogenesis. Hepatology 2015;61:214–226.

Supplementary Table 1. Sequences of Short Hairpin RNAs Used

Target	Sequences
Human-sh*ABL1*-1	CCGGGAGTTCTTGAAGCATTTCAAACTCGAGTTTGAAATGCTTCAAGAACTCTTTTTG
Human-sh*ABL1*-2	CCGGGCTTTGGGAAATTGCTACCTACTCGAGTAGGTAGCAATTTCCCAAAGCTTTTTG
Human-sh*NOTCH1*	CCGGCTTTGTTTCAGGTTCAGTATTCTCGAGAATACTGAACCTGAAACAAAGTTTTT

Supplementary Table 2. Primary Antibody Information

Antibody	Cat no.	Company
ABL1	2862	Cell Signaling
p-ABL1 (Tyr412)	2865	Cell Signaling
Phospho-AKT (Ser473)	4060	Cell signaling
AKT	9272	Cell Signaling
Phospho-ERK(Thr 202/Tyr 204)	4370	Cell Signaling
ERK	4695	Cell Signaling
NOTCH1	3608	Cell Signaling
Phospho-c-Myc (Ser62)	13748	Cell Signaling
c-MYC	5605	Cell Signaling
CRKL	3182	Cell Signaling
p-CRKL (Tyr207)	3181	Cell Signaling
GAPDH	G8795	Sigma
Ki67	RM-9106-S0	Fisher Scientific
NOTCH3	23426	Abcam
AFP	A0008	Dako

Supplementary Table 3. Primer Sequences Used for Reverse Transcription Polymerase Chain Reaction

Gene	Sequences
GAPDH-F	5′-CTCTGGAAAGCTGTGGCGTGATG-3′
GAPDH-R	5′-ATGCCAGTGAGCTTCCCGTTCAG-3′
NOTCH1-F	TGGACCAGATTGGGGAGTTC
NOTCH1-R	GCACACTCGTCTGTGTTGAC
NOTCH3-F	CGTGGCTTCTTTCTACTGTGC
NOTCH3-R	CGTTCACCGGATTTGTGTCAC
JAG1-F	GTCCATGCAGAACGTGAACG
JAG1-R	GCGGGACTGATACTCCTTGA
LFNG-F	GTCAGCGAGAACAAGGTGC
LFNG-R	GATCCGCTCAGCCGTATTCAT
DTX1-F	GACGGCCTACGATATGGACAT
DTX1-R	CCTAGCGATGAGAGGTCGAG
CCND1-F	GCTGCGAAGTGGAAACCATC
CCND1-R	CCTCCTTCTGCACACATTTGAA
Hes1-F	CCTGTCATCCCCGTCTACAC
Hes1-R	CACATGGAGTCCGCCGTAA
Hes2-F	CCAACTGCTCGAAGCTAGAGA
Hes2-R	AGCGCACGGTCATTTCCAG
NRARP-F	TCAACGTGAACTCGTTCGGG
NRARP-R	ACTTCGCCTTGGTGATGAGAT
NOTCH1 promoter-F	GAGCGCAGCGAAGGAACGA
NOTCH1 promoter-R	TCTCTTCCCCGGCTGGCT

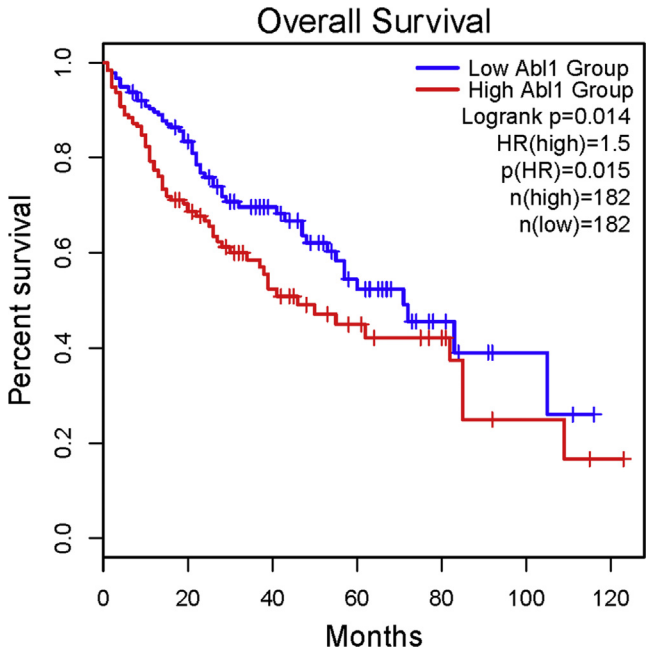

Supplementary Figure 1. High expression of *ABL1* in human HCCs is positively correlated with poorer patient prognosis. Kaplan-Meier plot of overall survival of HCC patients stratified by *ABL1* mRNA expression level from TCGA database.

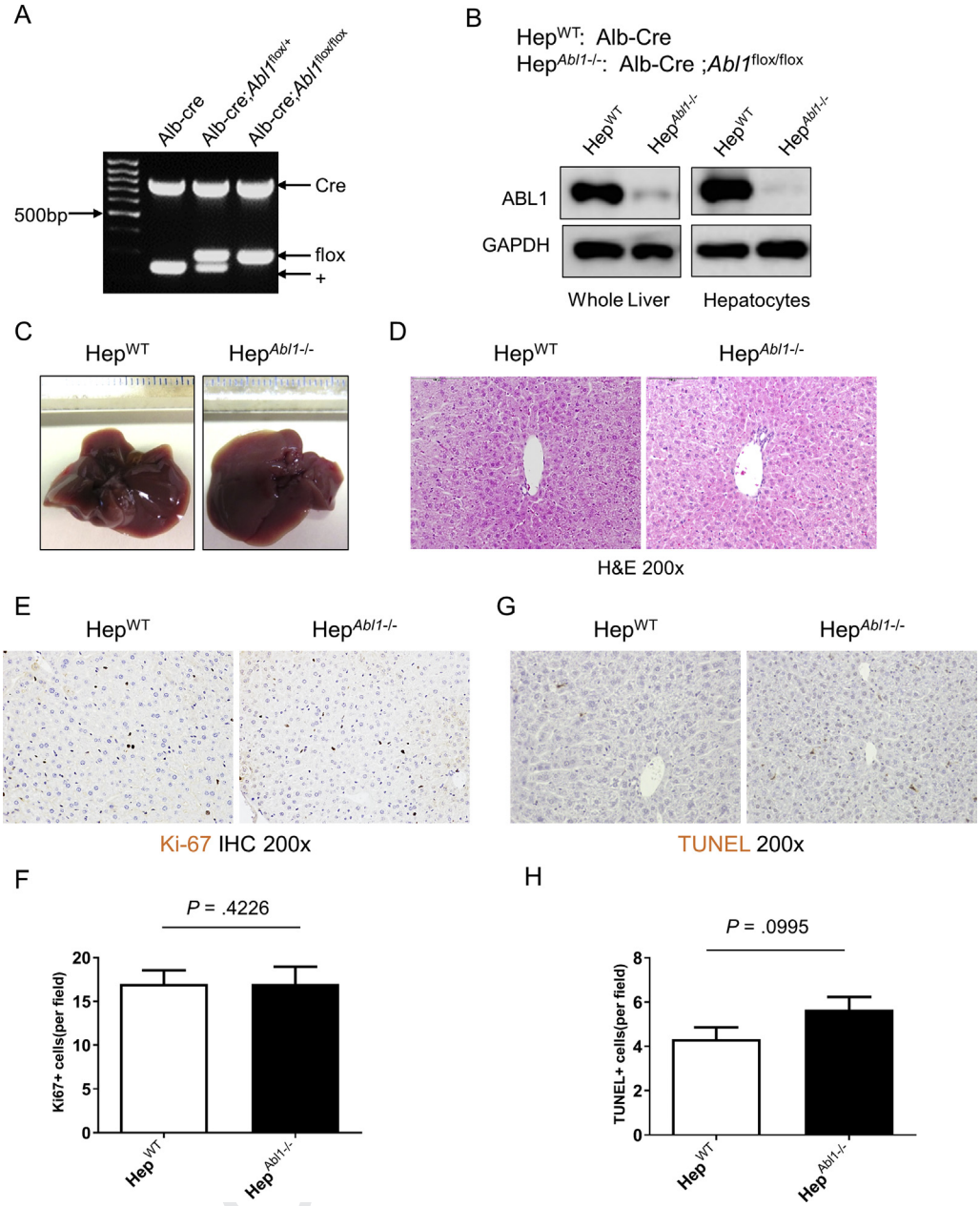

Supplementary Figure 2. Deletion of *Abl1* in hepatocytes does not affect morphology, histology, proliferation, or apoptosis in mouse liver. (*A*) Genotyping of Alb-Cre, Alb-Cre; *Abl1*$^{flox/+}$, and Alb-Cre; *Abl1*$^{flox/flox}$ mice. (*B*) Protein expression of ABL1 and GAPDH in whole liver tissues and isolated hepatocytes of Alb-Cre (Hep^{WT}) and Alb-Cre; *Abl1*$^{flox/flox}$ (Hep$^{Abl1-/-}$) mice was determined by Western blotting. (*C*) Photographs of livers from Hep^{WT} and Hep$^{Abl1-/-}$ mice at 7 weeks of age. (*D*) Representative pictures of H&E-stained sections for (*C*). (*E*) Hepatic proliferation in the livers of 7-week-old Hep^{WT} and Hep$^{Abl1-/-}$ mice was examined by immunohistochemistry for Ki67 protein expression. (*F*) Quantification of Ki67 staining (n = 4). (*G*) Hepatic apoptosis in the livers of 7-week-old Hep^{WT} and Hep$^{Abl1-/-}$ mice was examined by TUNEL staining. (*H*) Quantification of TUNEL staining for (*G*) (n = 4).

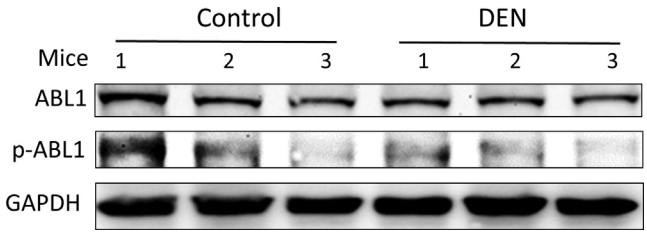

Supplementary Figure 3. *ABL1* is not activated in diethylnitrosamine (DEN)-induced HCC tumors. Expression of p-ABL1, ABL1, and GAPDH proteins in the livers of wild-type C57B6/J male mice 10 months after injection of DEN.

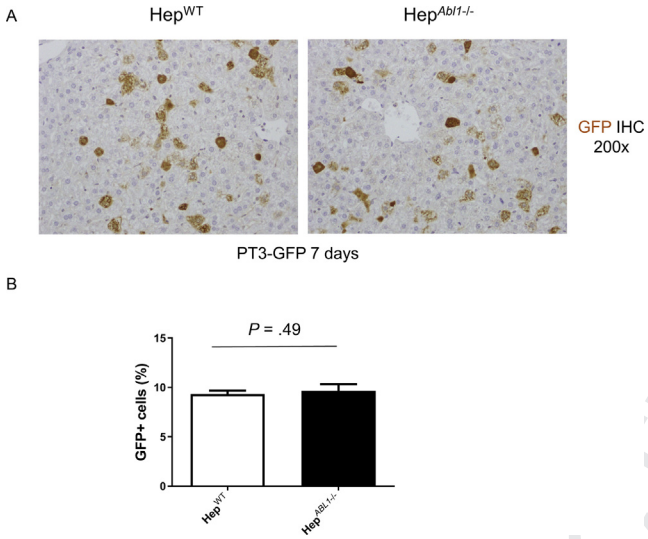

Supplementary Figure 4. Comparable transfection efficiency of hydrodynamic injection in WT and *Abl1*-KO mouse liver. (*A*) GFP expression in the livers of 7-week-old Hep^{WT} and Hep$^{Abl1-/-}$ mice (n = 3/group) was examined by immunohistochemistry 7 days after injection of pT3-GFP. (*B*) Quantification of GFP staining (n = 3/group).

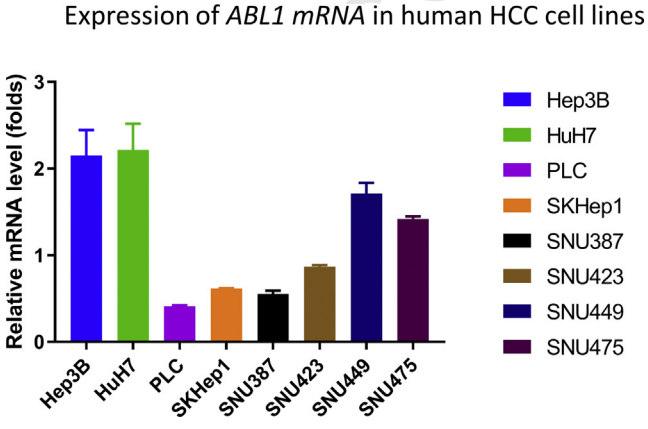

Supplementary Figure 5. *ABL1* is expressed in HCC cells. Relative *ABL1* mRNA levels in a number of HCC cell lines were examined by real-time polymerase chain reaction.

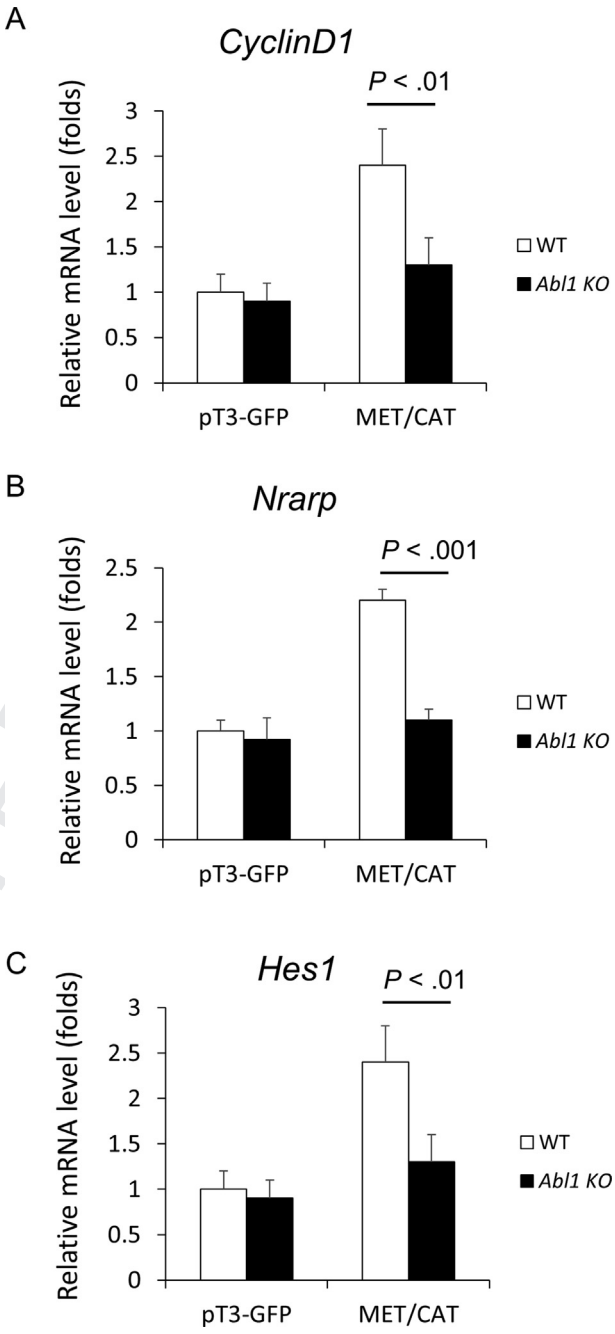

Supplementary Figure 6. Knockout of *ABL1* decreases expression of NOTCH1 targets in MET/CAT-induced HCC tumors. (*A–C*) Relative *CyclinD1, Nrarp,* and *Hes1* mRNA levels in whole livers of Hep^{WT} and Hep$^{Abl1-/-}$ mice treated with pT3-GFP or MET/CAT for 9 weeks was determined by real-time polymerase chain reaction.

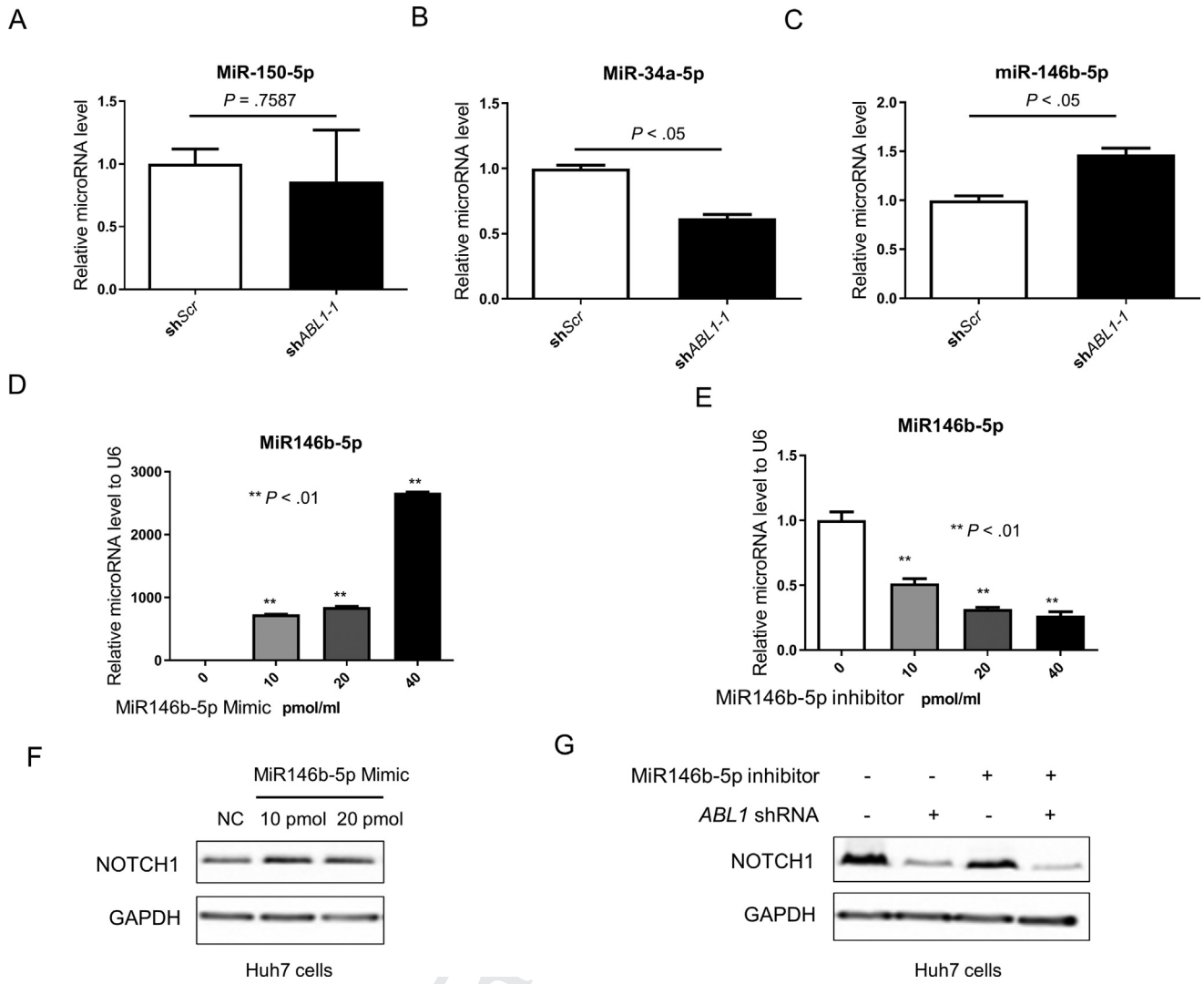

Supplementary Figure 7. miRs may not contribute to regulation of *NOTCH1* by ABL1. (*A*) Relative *miR-150-5p* mRNA levels in scrambled-RNA and *ABL1*-KD Huh7 cells. (*B*) Relative *miR-34a-5p* mRNA levels in scrambled-RNA and *ABL1*-KD Huh7 cells. (*C*) Relative *miR-146b-5p* mRNA levels in scrambled-RNA and *ABL1*-KD Huh7 cells. (*D*) Relative *miR-146b-5p* levels in Huh7 cells treated with miR146b-bp-mimic at different concentrations. (*E*) Relative *miR-146b-5p* levels in Huh7 cells treated with miR146b-bp inhibitors at different concentrations. (*F*) Expression of NOTCH1 and GAPDH proteins in Huh7 cells treated with control or *miR146b-5p-mimic* for 24 hours. (*G*) Expression of NOTCH1 and GAPDH proteins in scrambled-RNA and *ABL1*-KD Huh7 cells treated with control or *miR146b-5p* inhibitors for 24 hours.

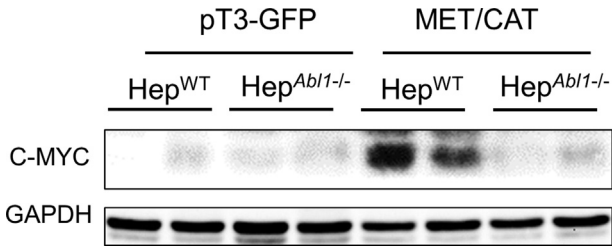

Supplementary Figure 8. Knockout of *ABL1* decreases expression of c-MYC in MET/CAT-induced HCC tumors. c-MYC expression in whole livers of Hep^{WT} and $Hep^{Abl1-/-}$ mice treated with pT3-GFP or MET/CAT for 9 weeks was determined by Western blotting.

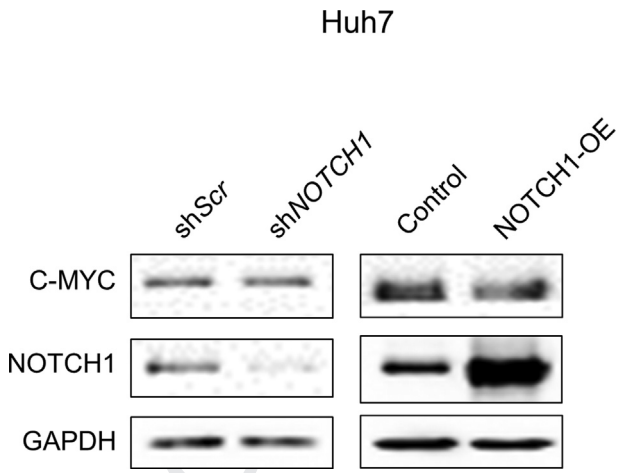

Supplementary Figure 10. Neither knockdown nor overexpression of *NOTCH1* affects expression of c-MYC protein in HCC cells. Expression of c-MYC, NOTCH1, and GAPDH proteins in Huh7 cells infected with scrambled-shRNA, NOTCH1-shRNA, EF.CMV.GFP (control), or EF.hICN1.CMV.GFP (NOTCH1-OE).

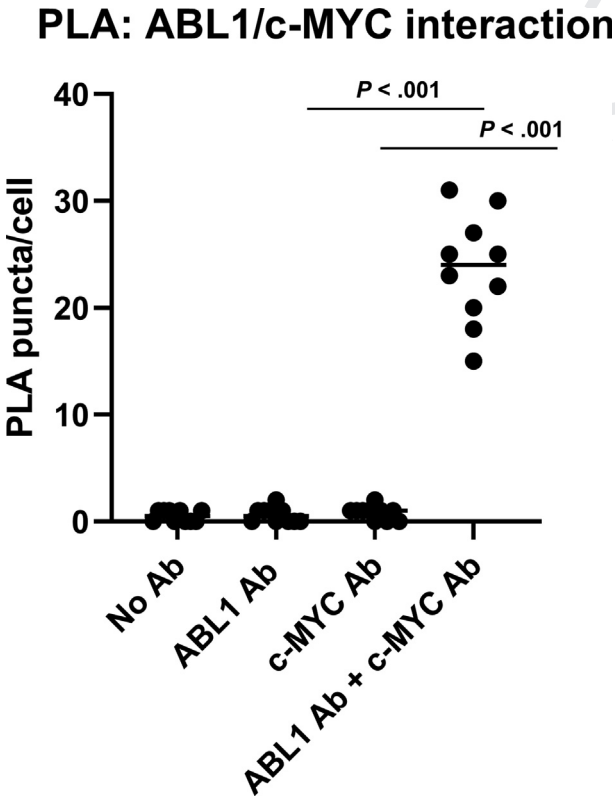

Supplementary Figure 9. ABL1 interacts with c-MYC in HCC cells. The interaction of ABL1 and c-MYC was examined using proximity ligation assay (PLA) in Huh7 cells. PLA puncta per cell was quantified using Image J software (National Institutes of Health, Bethesda, MD).

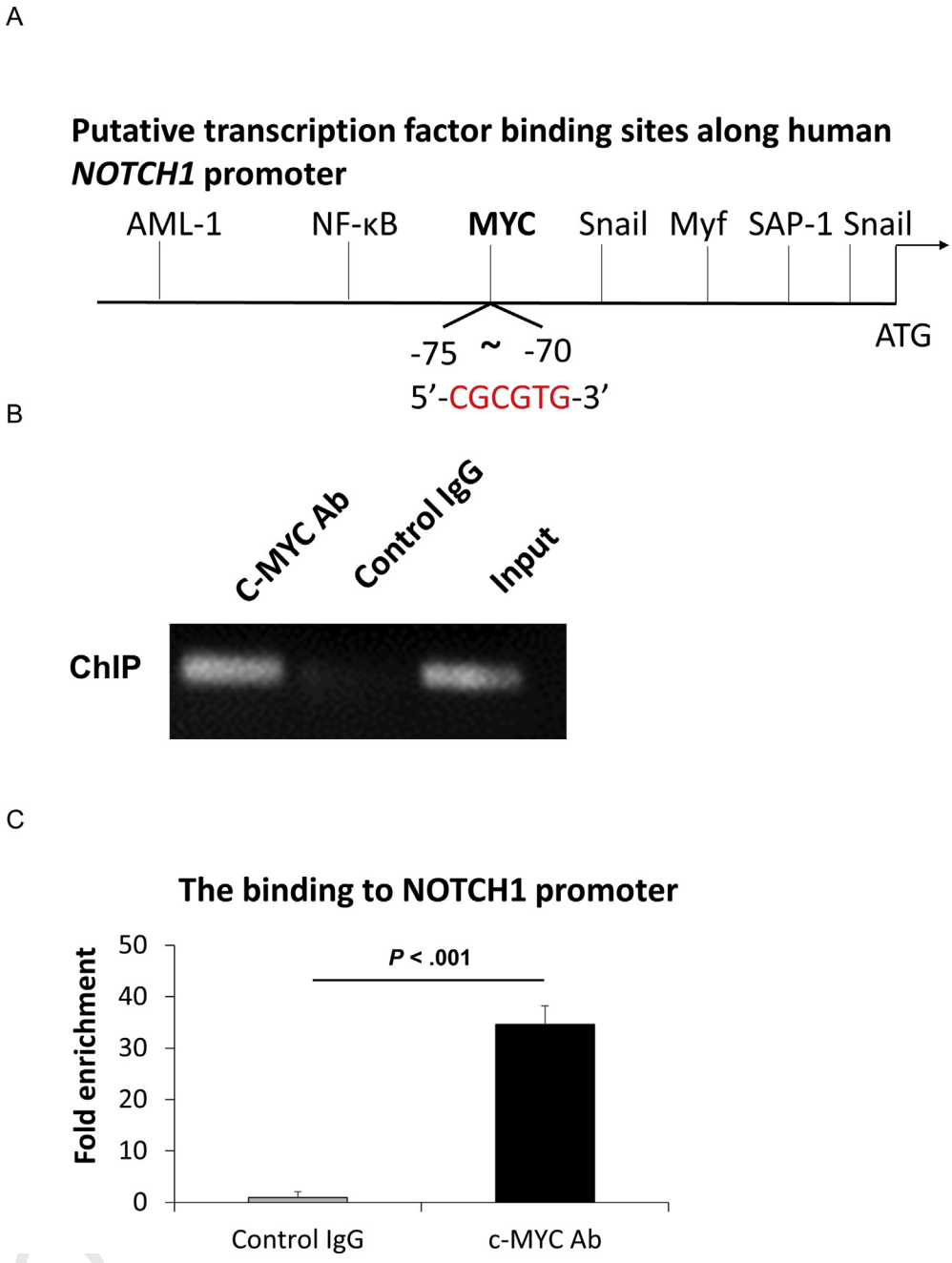

Supplementary Figure 11. c-MYC directly binds to the promoter of *NOTCH1* in human HCC cells. (*A*) Putative transcription factor binding sites human *NOTCH1* promoter were analyzed by TFsearch software. (*B*) Chromatin immunoprecipitation (ChIP) polymerase chain reaction (PCR) analysis reveals the binding of c-MYC to the *NOTCH1* promoter in Huh7 cells. (*C*) ChIP- quantitative PCR analysis reveals the binding of c-MYC to the *NOTCH1* promoter in Huh7 cells.

A

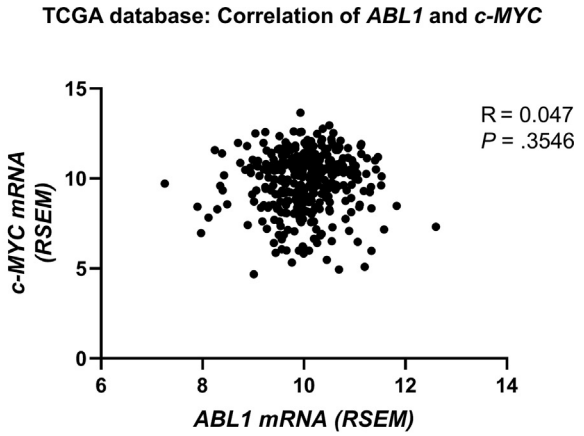

B

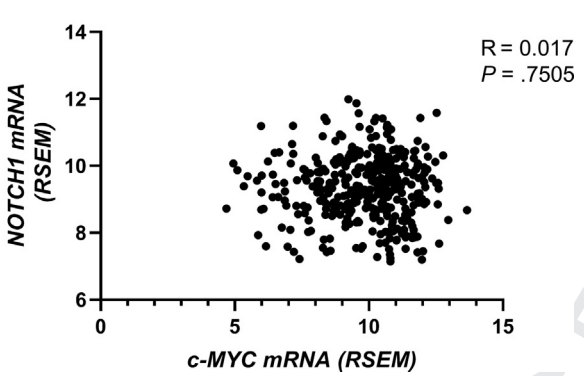

Supplementary Figure 12. *c-MYC* mRNA level has no correlation with *ABL1* or *NOTCH1* mRNA levels in TCGA HCC samples. (*A*) Correlation of *c-MYC* and *ABL1* mRNA in HCC samples from the TCGA database was analyzed. (*B*) Correlation of *c-MYC* and *NOTCH1* mRNAs in HCC samples from the TCGA database was analyzed.

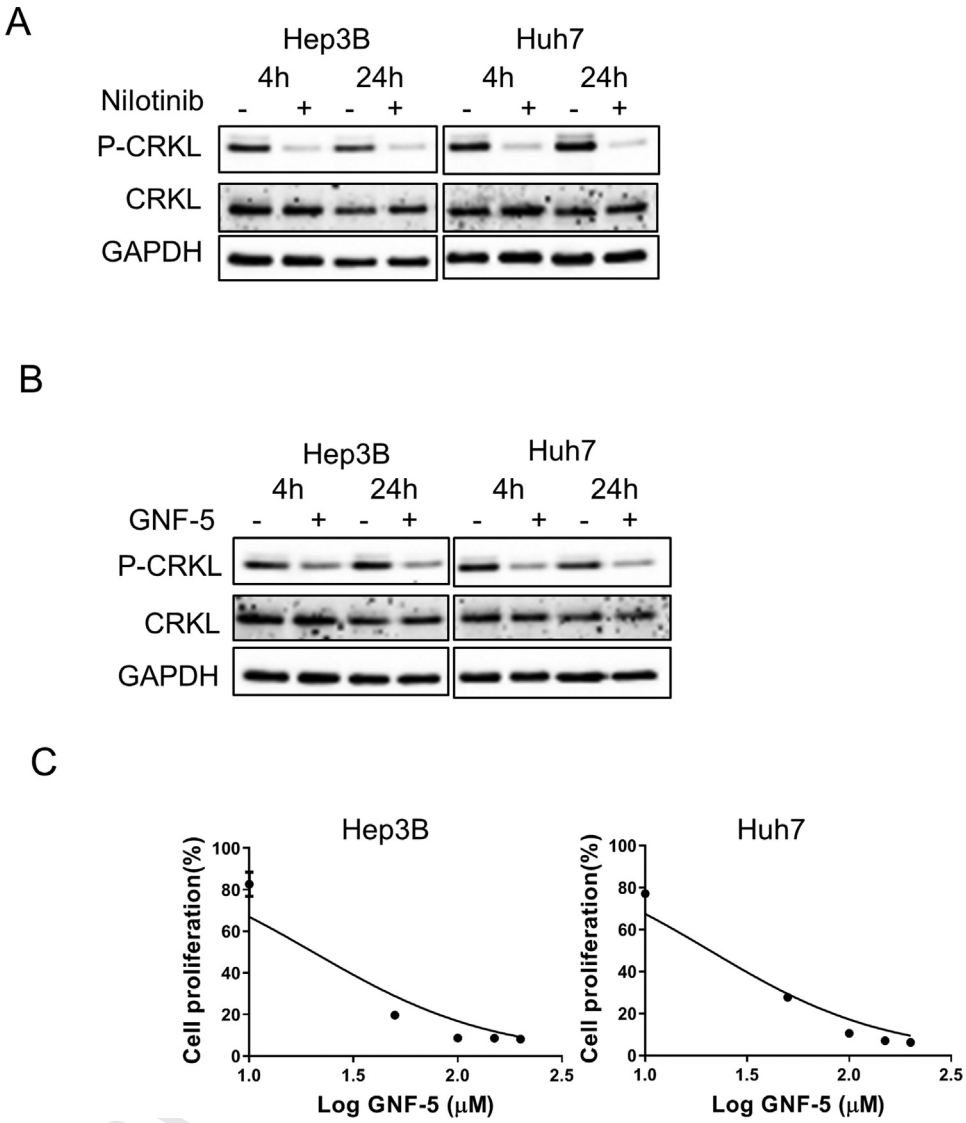

Supplementary Figure 13. ABL inhibitors inhibit HCC cell growth. (*A*) Expression of p-CRKL (a direct target of ABL1), CRKL, and GAPDH proteins in Hep3B and Huh7 cells treated with vehicle or 3 μM nilotinib for 4 hours or 24 hours. (*B*) Expression of p-CRKL, CRKL, and GAPDH proteins in Huh7 cells treated with vehicle or 20 μM GNF5 for 4 hours or 24 hours. (*C*) Quantification of cell proliferation of Hep3B and Huh7 cells treated with vehicle or GNF-5 at different time points after treatment.

A **IC50 for Nilotinib**

Cell lines	Hep3B	SK-Hep1	Huh7	SNU-423	SNU-449	SNU-475	PLC/PRF/5	SNU-387
IC50 (μM)	5.02	6.15	5.88	11.03	11.69	6.93	11.2	10.2

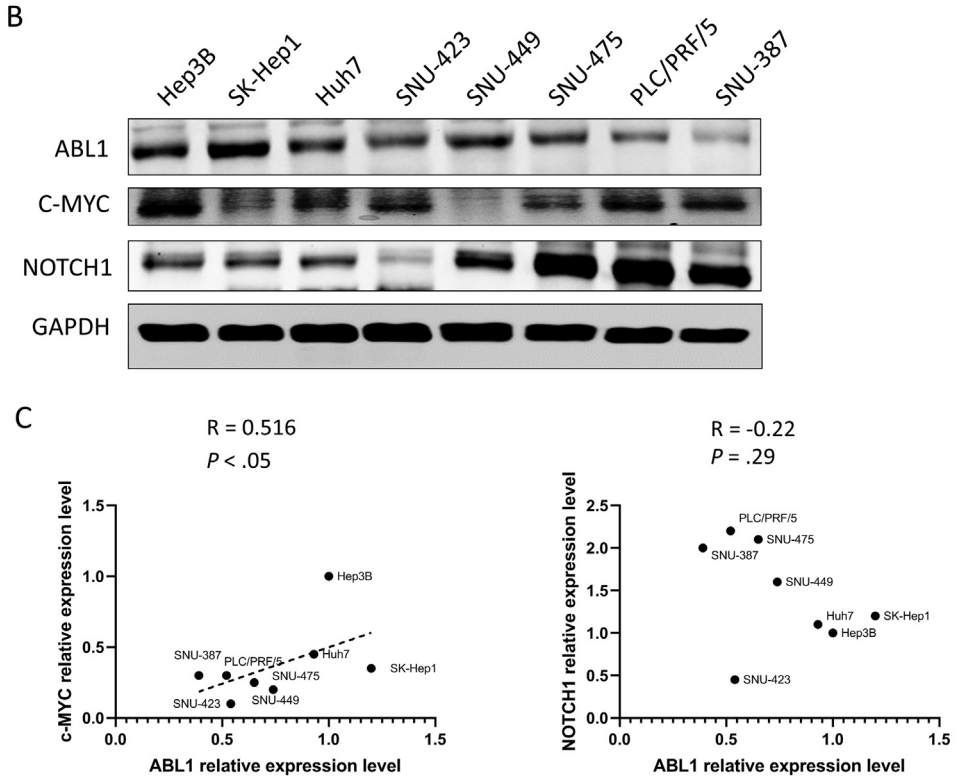

Supplementary Figure 14. Nilotinib treatment decreases HCC cell growth. (*A*) 50% inhibitory concentration (IC50) for nilotinib in 8 HCC cell lines was calculated for cell growth experiment described in Figure 7*A* using nonlinear regression. (*B*) Expression of ABL1, c-MYC, NOTCH1, and GAPDH proteins in 8 HCC cells. (*C*) Correlation between c-MYC (*left*) and NOTCH1 (*right*) protein expression and ABL1 protein expression in 8 HCC cell lines. (*D*) Correlation between NOTCH1 protein expression and ABL1 protein expression in HCC cells with or without p53 mutations.

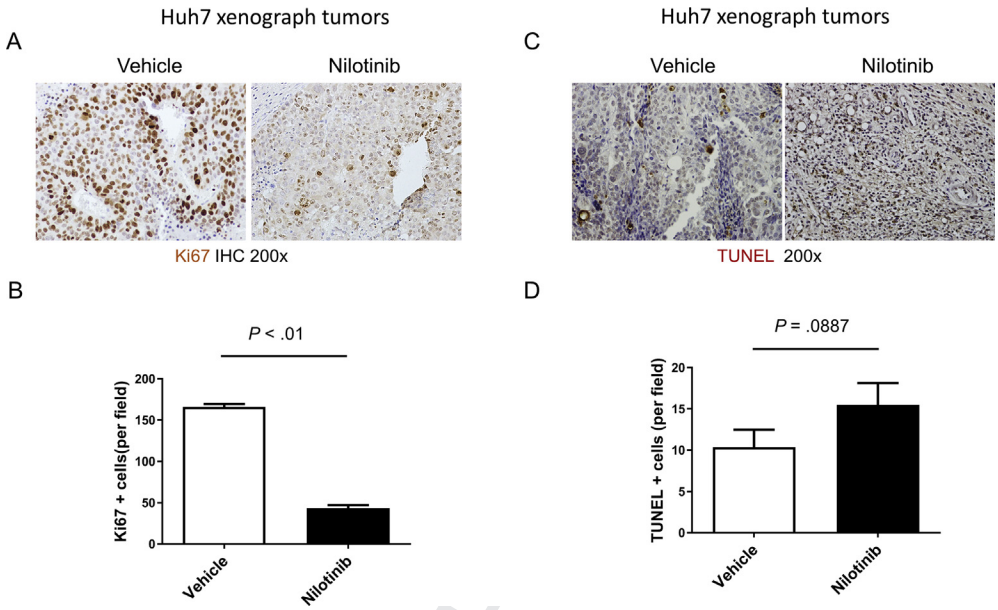

Supplementary Figure 15. Nilotinib treatment decreases HCC cell proliferation in a xenograft model. (*A*) Ki67 staining of tumors from Huh7 cells treated with vehicle or nilotinib was examined by IHC. (*B*) Quantification of Ki67 staining (n = 3/group). (*C*) TUNEL staining of Huh7 xenograft tumors treated with vehicle or nilotinib was examined by IHC. (*D*) Quantification of TUNEL staining (n = 3/group).

web 4C/FPO

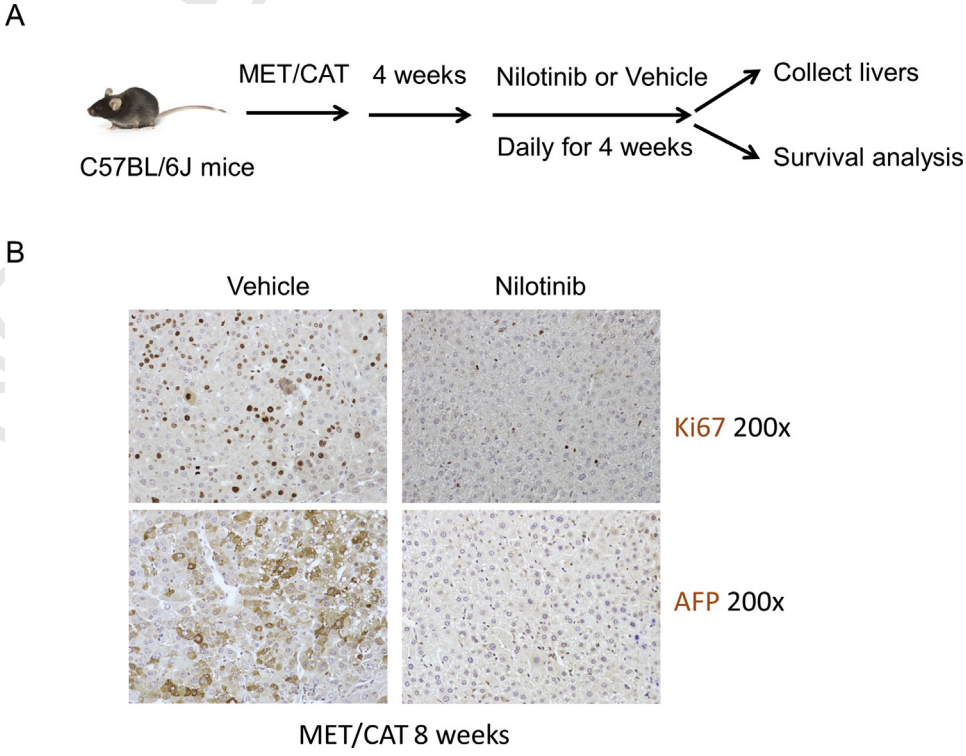

Supplementary Figure 16. Nilotinib treatment decreases HCC cell proliferation in the MET/CAT model. (*A*) Diagram of the experimental protocol. (*B*) Ki67 and AFP staining of tumors induced by MET/CAT treated with vehicle or nilotinib was examined by IHC.

web 4C/FPO

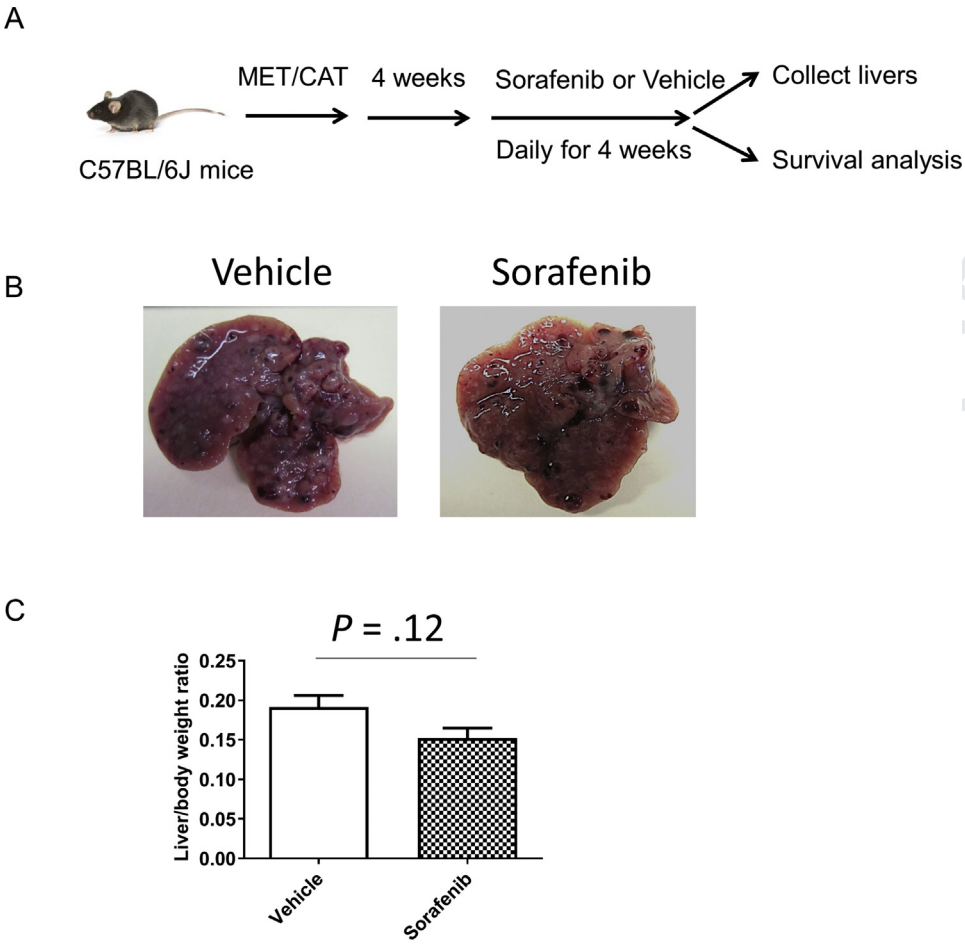

Supplementary Figure 17. Sorafenib is not effective in suppressing tumor growth in the MET/CAT-induced HCC model. (*A*) Diagram of the experimental protocol. (*B*) *Gross images* of tumors from vehicle- (*left*) and sorafenib-treated animals (*right*) are shown. (*C*) Body weight ratios of mice after/before sorafenib treatment (n = 6/group). (*D*) Kaplan-Meier survival *graph* for mice treated with vehicle or sorafenib (n = 6/group).

web 4C/FPO

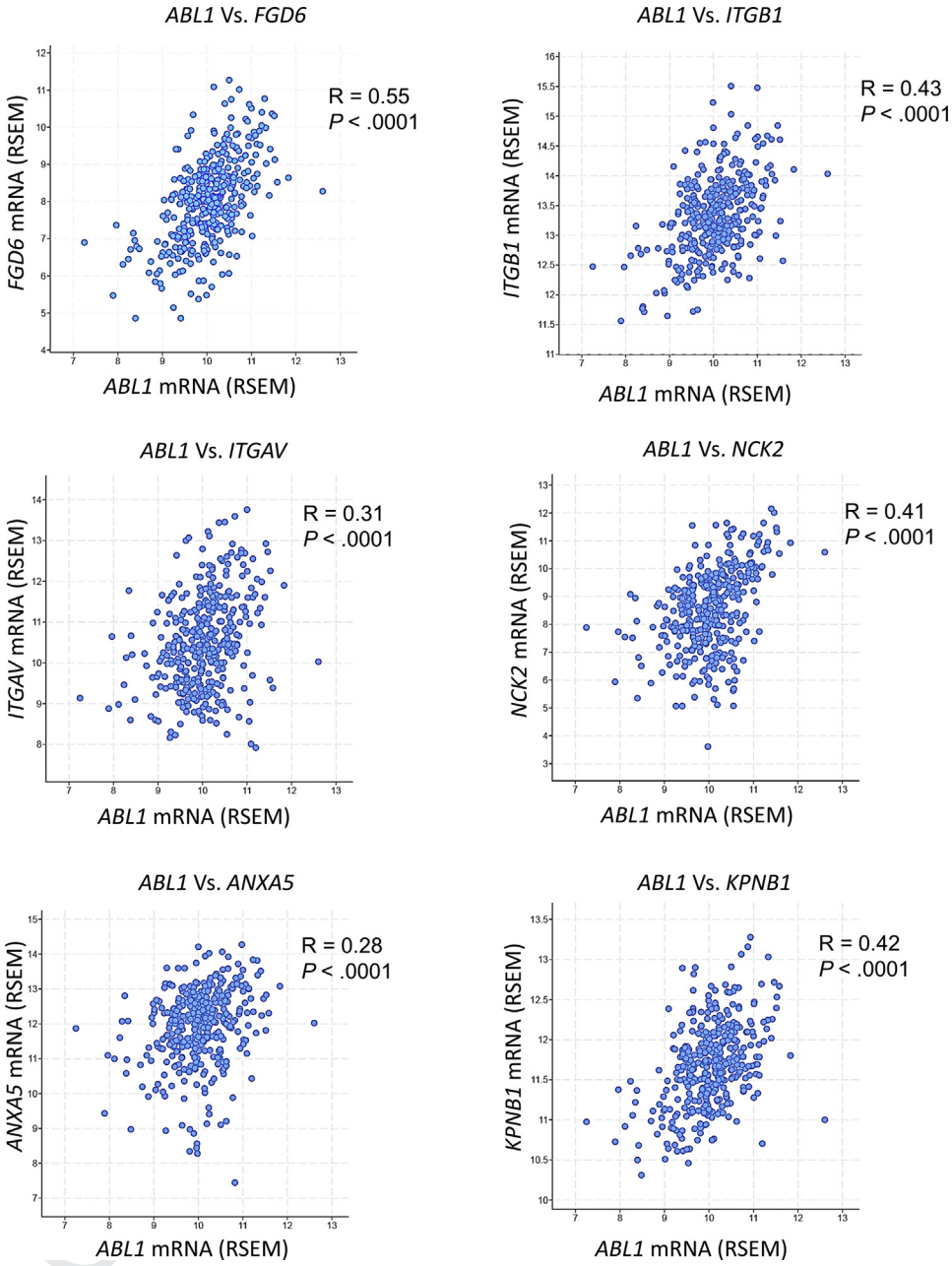

Supplementary Figure 18. *ABL1* expression is correlated with expression of c-MET–activated genes. Correlation between *ABL1* mRNA expression and the expression of genes (*FGD6, ITGB1, ITGAV, NCK2, ANXA5,* and *KPNB1*) from "the c-MET activation gene set" in human HCCs from TCGA database.

web 4C/FPO

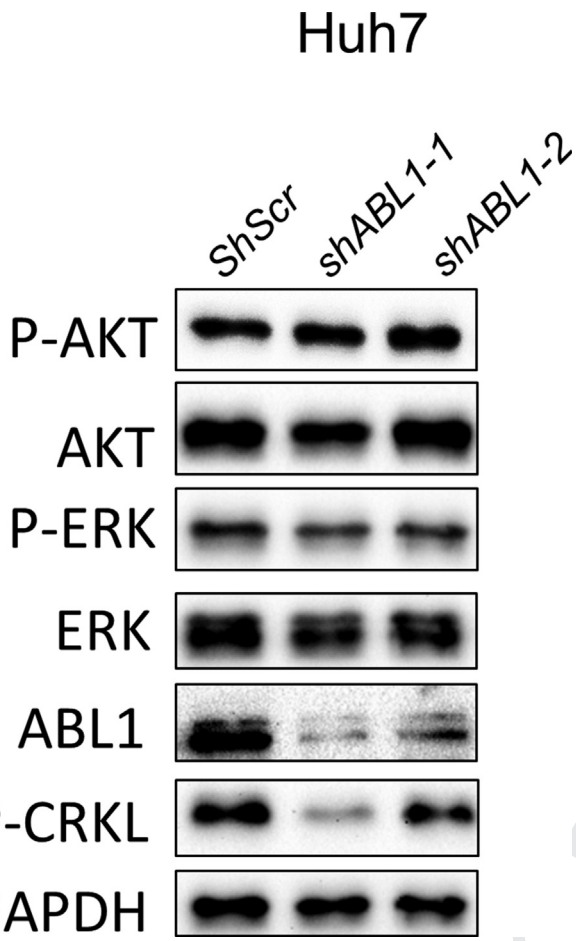

Supplementary Figure 19. Neither knockdown nor overexpression of *NOTCH1* affects phosphorylation of AKT or ERK in HCC cells. Expression of p-AKT, AKT, p-ERK, ERK, ABL1, p-CRKL, and GAPDH proteins in Huh7 cells infected with scrambled-RNA or *ABL1*-KD Huh7 cells.

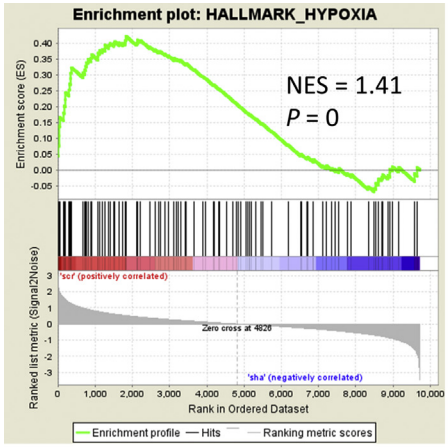

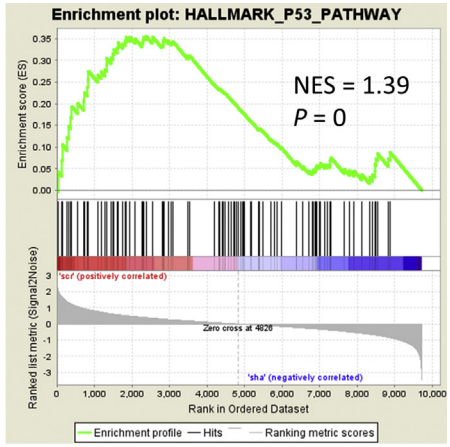

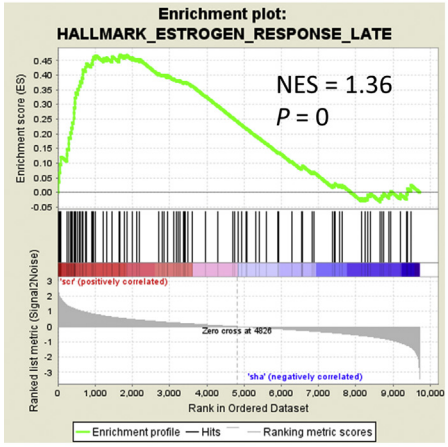

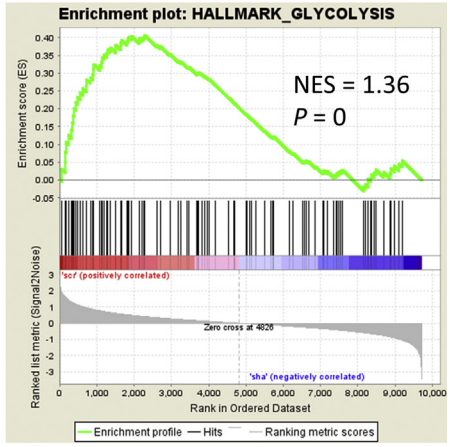

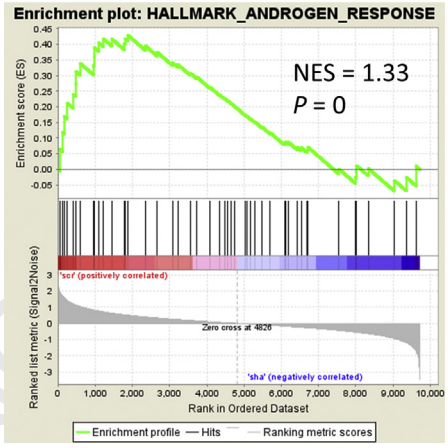

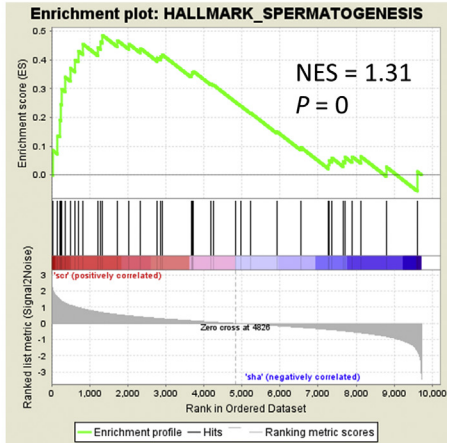

Supplementary Figure 20. *ABL1* knockdown down-regulates a number of signaling pathways. GSEA reveals down-regulation of several gene sets, including hypoxia, the p53 pathway, estrogen response, glycolysis, androgen response, and spermatogenesis by knockdown of *ABL1* in Huh7 cells.